

**IMPROVEMENT OF INTERFACIAL TOUGHNESS OF
LAYERED COMPOSITES BY USING ELECTROSTATIC
FLOCKING TECHNIQUE**

**ELEKTROSTATİK FLOKLAMA TEKNİĞİ
KULLANILARAK KATMANLI KOMPOZİTLERİN
ARAYÜZ TOKLUĞUNUN GELİŞTİRİLMESİ**

MUSTAFA UTKU YILDIRIM

PROF. DR BORA MAVİŞ

Supervisor

Submitted to

Graduate School of Science and Engineering of Hacettepe University

as a Partial Fulfillment to the Requirements

for the Award of Degree of Master of Science in Mechanical Engineering

ABSTRACT

IMPROVEMENT OF INTERFACIAL TOUGHNESS OF LAYERED COMPOSITES BY USING ELECTROSTATIC FLOCKING TECHNIQUE

Mustafa Utku Yıldırım

Master of Science, Department of Mechanical Engineering

Supervisor: Prof. Dr. Bora MAVİŞ

Co- Supervisor: Assoc. Prof. Dr. Erhan BAT

June 2021, 62 pages

Fiber-reinforced composites have remarkable strength to weight ratio. Hence, their areas of usage are increasing. Solving the delamination problem that affects service life of layered composites has gained importance. As a solution, addition of toughening particles or interleaves (in the form of films or nanofibrous veils laid parallel to the layers) to the brittle interlayer matrix material have been proposed. Z-pinning applied perpendicular and across the whole lamina is another method. It is known that nanofibers of the veils or the pins activate bridging mechanisms between adjacent layers during crack propagation. For the same purpose, perpendicular placement of small chopped fibers (flock) to the interface was experimented by electrostatic flocking, which is mechanism-wise similar to the z-pinning method, but akin to interleaving with veils in terms of the location of modification. In previous studies, the possible advantage of using shorter Nylon 66 (N66) flocks in interlayer modification was demonstrated using 1.3 mm flocks.

In this study, it is hypothesized that the use of flocks with sizes approaching the similar size scale of the hills and troughs forming among the twills of the epoxy impregnated carbon fiber fabric (prepreg) can increase the effectiveness of the flocks in their vertical bridging positions. In addition, commercial flocks which have been used at the composite interface had never been functionalized with the purpose of improving the matrix – flock interface, as far as the available literature concerned.

Here, 0.4 mm long 0.9 dtex N66 flocks, with or without an amino silane modification, were coated on prepreg surfaces with variable densities and vertical alignments under the effect of different voltage, time and distance values during flocking. In the control of areal density and obtaining maximum vertical alignment, the total flight distance was found to be more effective than the other process parameters.

Mode I interlaminar toughness values of the produced composites were determined. The amino silane-treated N66 flocks which showed the highest increases showed an 18% increase in the G_{IC} initiation value and a 35% increase in the G_{IC} propagation value relative to the unflocked reference sample. Examination of the delaminated surfaces after double cantilever beam (DCB) tests with scanning electron microscope (SEM) revealed the fact that N66 flocks were able to activate a debonding based toughening mechanism, but prone to easy-peeling due to insufficient chemical interaction with the matrix epoxy. On the other hand, amino functionalities in the modified flocks increased the debonding resistance and led to bridging mode failure upon this debonding that was becoming harder. With further modifications to the surface treatment and mechanical test procedures, higher gains in interlaminar toughness values can be expected.

Keywords: electrostatic flocking, flock, N66, carbon fiber, epoxy, layered composite, interface, toughening mechanism

ÖZET

ELEKTROSTATİK FLOKLAMA TEKNİĞİ KULLANILARAK KATMANLI KOMPOZİTLERİN ARAYÜZ TOKLUĞUNUN GELİŞTİRİLMESİ

Mustafa Utku YILDIRIM

Yüksek Lisans, Makine Mühendisliği Bölümü

Tez Danışmanı: Prof. Dr. Bora MAVİŞ

Eş Danışman: Doç.Dr. Erhan BAT

Haziran 2021, 62 sayfa

Fiber takviyeli kompozit malzemeler, düşük özgül ağırlıkları yanında yüksek mukavemet göstermektedir. Bu nedenle kullanım alanları gün geçtikçe artmaktadır. Tabakalı kompozitlerin kullanım ömrüne etki eden delaminasyon problemine çözüm üretmek önem kazanmıştır. Çözüm olarak, arayüzdeki gevrek matrise; toklaştırıcı parçacık veya tabakalara paralel ek film veya fiberlerden oluşan tül tabakası eklenmesi önerilmektedir. Tabakalara dik yönde boydan boya uygulanan z-pimleme metodu ise bir diğer yöntemdir. Tülleri oluşturan nanofiberlerin veya pimlerin çatlak ilerlemesi sırasında bitişik tabakalar arasında köprüleme mekanizmalarını etkinleştirdiği bilinmektedir. Benzer amaç için, mekanizma olarak z-pimleme metoduna benzetilebilecek, ancak eklentinin yapıldığı yer olarak tül eklemeye benzeşen, elektrostatik floklamayla; arayüze dik olarak küçük fiber parçalarının (flok) yerleştirilmesi denenmiştir. Daha önceki çalışmalarda, katmanlar arası modifikasyonda daha kısa Naylor 66 (N66) flokların kullanılmasının olası avantajı, 1.3 mm boyunda floklar kullanılarak gösterilmiştir.

Bu çalışmada; floklama işleminde, epoksi emdirilmiş karbon fiber kumaşın (prepreg) örgü "tepe ve olukları" nın boyut ölçeğine yaklaşan flokların kullanılmasının, flokların dikey köprüleme konumundaki etkinliklerini arttırabileceği öngörülmüştür. Ayrıca literatürde daha önce arayüze yerleştirilen ticari flokların yüzeylerine, matris – flok etkileşimini arttırmak üzere bir işlevselleştirme işlemi uygulanmamıştır.

Çalışma kapsamında; 0.4 mm boyundaki 0.9 dtex N66 floklar, herhangi bir yüzey modifikasyonu olmadan ya da bir amino silan molekülüyle işlevselleştirildikten sonra, floklama sırasında uygulanan farklı voltaj, süre ve uzaklık değerleriyle, prepreg yüzeylerine değişen yoğunluk ve dikliklerde yerleştirilmiştir. Flokların yüzey alan yoğunluğunun kontrolünde ve maksimum diklik oranlarının elde edilmesinde toplam uçuş mesafesinin diğer işlem parametrelerinden daha etkin olduğu tespit edilmiştir.

Oluşturulan kompozitlerin Mod I arayüz toklukları belirlenmiştir. En yüksek artışların sağlandığı, işlevselleştirilmiş N66 floklarla üretilmiş kompozitlerde, flok eklenmemiş referans numunesine göre G_{IC} başlangıç ve G_{IC} ilerleme değerinde, sırasıyla %18 ve %35 artış elde edilmiştir. Çift ankastre giriş (DCB) testi sonrası ayrılma yüzeylerinin taramalı elektron mikroskobu (SEM) görüntüleri incelendiğinde; N66 flokların çatlak ilerlemesine karşı bağaçımı mekanizmasını etkinleştirdiği, ancak matris epoksisıyla yetersiz bir kimyasal etkileşim göstermeleri nedeniyle, kolay sıyrılmaya açık hale geldikleri görülmüştür. Diğer yandan, yüzeyleri donanmış floklardaki amino işlevsel gruplar bağaçımını zorlaştırmış ve bu zorlaşan bağaçımı ardına köprüleme pozisyonunda kopmalara yol açmıştır. Yüzey işlemi ve mekanik test prosedürüne yapılacak iyileştirmelerle, arayüz tokluk değerlerinde daha yüksek artışların sağlanması beklenmektedir

Anahtar Kelimeler: elektrostatik floklama, flok, N66, karbon fiber, epoksi, tabakalı kompozit, arayüz, toklaştırma mekanizması

ACKNOWLEDGEMENTS

I would like to thank Prof. Dr. Bora Maviş for his continuous support during my graduate education. This made me feel that he is always with me. He not only shaped my scientific point of view, but also my life and became my mentor with his profound knowledge and experience. I am also grateful to my honorable co-advisor Assoc. Prof. Dr. Erhan BAT, for his immediate support whenever I needed and the deep chemistry insight he provided in the surface treatment of flocks.

I am privileged to meet and work with Kamil URGUN and Öznur DOĞAN as my lab mates, who helped me with the tedious and time-consuming laboratory chores.

And my dear family... You supported me through my life under every circumstance, showed patience and always put my priorities before yours. This, I will never be able to repay completely. You have made the greatest of all contributions to me until now. I will never give up any moment of my life with you, for anything else in this life.

Many Thanks!

I also acknowledge use of the services and facilities of UNAM-National Nanotechnology Research Center at Bilkent University.

Hacettepe University (Grant Number: FYL-2020-18719) and Turkish Scientific and Technical Research Council – TÜBİTAK (Grant Number: 214M110) provided the financial support for the completion of this thesis.

Mustafa Utku YILDIRIM

June 2021, Ankara

TABLE OF CONTENTS

ABSTRACT	i
ÖZET.....	iii
ACKNOWLEDGEMENTS	v
TABLE OF CONTENTS	vi
TABLE OF FIGURES	viii
LIST OF TABLES	x
SYMBOLS AND ABBREVIATIONS	xi
1. INTRODUCTION.....	1
2. LITERATURE SURVEY	4
2.1. Composite Materials	4
2.2. Composite Materials Damage Modes	5
2.3. Methods to Increase Delamination Resistance.....	10
2.4. Electrostatic Flocking.....	13
3. EXPERIMENTAL STUDIES	18
3.1. Materials 18	
3.1.1 Flocks	18
3.1.2 Surface Treatment of Flocks	18
3.1.3 Prepreg	19
3.2. Electrostatic Flocking Application Cabin	19
3.3. Flocking Setup for Interfacial Engineering of Layered Composites.....	20
3.4. Lay-up Process	22
3.5. Mechanical Test for Mode I Fracture Toughness	23
3.6. Material Characterization	24
3.6.1 Scanning Electron Microscope (SEM).....	24
3.6.2 Fourier-Transform Infrared Spectroscopy (FT-IR).....	25
4. RESULTS AND DISCUSSION	26

4.1. Electrostatic Flocking Studies	26
4.1.1. Controlling the Areal Density of 0.6 mm 1.7 dtex N66 Flocks.....	26
4.1.2. Controlling the Areal Density of 0.4 mm 0.9 dtex N66 Flocks.....	28
4.2. Mode I Fracture Toughness Tests of Laminates.....	32
4.2.1 Reference Laminates.....	32
4.2.2 0.4 mm N66 Flocked Composites (R42-N66).....	35
4.2.2 Silane Treated N66 Flocked Composites (R42-N66-S)	39
5.CONCLUSIONS	44
6. REFERENCES	46
APPENDIX.....	49
APPENDIX 1 – Example of DCB test data processed according to ASTM-D5528..	49
APPENDIX 2 – Determination of flock density and vertical alignment on the prepreg	54
APPENDIX 3– Presentations from Thesis	60
APPENDIX 4 - Thesis Originality Report	61
PERSONAL BACKGROUND.....	62

TABLE OF FIGURES

Figure 1	Interaction of a bridging fiber with the crack front. (a) Schematic view of an embedded fiber interacting with the crack front, which can result in (b) straining of the fiber without debonding, (c) straining of the nanofiber with partial debonding from the epoxy, or (d) complete debonding of the nanofiber (peeling). [12].....	2
Figure 2	Schematic Diagram of Flocking Between 2 Layer [9].....	3
Figure 3	Typical reinforcement types [16].....	4
Figure 4	Lamina and Laminate lay-ups [3].....	5
Figure 5	Schematic damage modes in CFRP laminate [6].....	6
Figure 6	Various cracking modes for fracture toughness classification [4].	6
Figure 7	Double Cantilever Beam Specimen[19].....	7
Figure 8	Delamination Resistance Curve (R Curve) from DCB Test [19].....	8
Figure 9	Load Displacement Trace from DCB Test [19].	9
Figure 10	Modified Beam Theory [19].....	10
Figure 11	DC Flocking Process [28]	14
Figure 12	Arrangement of (a) N66 fibers, (b) PCFs (PAN-based carbon fiber) and (c) mPCFs (mesophase pitch-based carbon fibers) after electrostatic flocking [29].	15
Figure 13	Aminosilane treatment.	19
Figure 14	ommercial electrostatic flocking cabin.	20
Figure 15	Designed flock cabin.	21
Figure 16	Frame for prepreg.....	21
Figure 17	Teflon band and continuous film laid prepregs (9 layer side).	22
Figure 18	Curing cycle.....	23
Figure 19	Test coupon placed in mechanical test machine and camera used for crack capturing.	24
Figure 20	Framed carbon fiber prepreg with SEM coupon positions on it.	25
Figure 21	Illustration of setup, X: distance between grid and top plate, Y: distance between the grid and bottom plate	26
Figure 22	VA and areal density changes with respect to electric field for 0.4 mm N66 flocks (time is constant in all experiments).....	29
Figure 23	VA and areal density changes with respect to flight distance and more specifically X (distance between grid to top plate) for 0.4 mm N66 flocks (time and voltage is constant in all experiments).	29
Figure 24	SEM images of 0.4 mm N66 flocks on prepreg surface; A-B (93 flocks/mm ² – 63% VA), C-D (155 flocks/mm ² – 38% VA), E-F (87 flocks/mm ² – 44%VA).....	31
Figure 25	Load – displacement curve of the 1 st reference plate using Teflon band (R42-B1). ..	32
Figure 27.	Load displacement curve of the 2nd reference plate using teflon band(R42-B2).	33

Figure 28	Load displacement curve of the reference plate using continuous film (R42-CF).....	33
Figure 29	Variations of G_{IC} values of reference plates with crack length.	34
Figure 30	SEM image of fracture interfaces of reference plates (R42-B1), A ($\times 140$), B ($\times 600$).35	
Figure 31	Load displacement curve of N66-VA1.....	35
Figure 32	Load displacement curve of N66-VA2.....	36
Figure 33	Load displacement curve of N66-VA3.....	36
Figure 34	SEM images of fracture interface of 0.4 mm N66 flocked prepreg, A and B from bottom surface (flocked), C and D from top surface.....	38
Figure 35	Load displacement curve of N66-S1-VA2.....	39
Figure 36	Load displacement curve of N66-S2-VA2.....	39
Figure 37	Load displacement curve of N66-S2-VA3.....	40
Figure 38	FTIR results of N66 flocks and all steps of silanization.....	41
Figure 39	SEM images of silane treated N66 flocked laminate's fracture surface.	43
Figure 40	Painted DCB coupon.....	49
Figure 41	Sample inserting to mechanical testing device.....	50
Figure 42	Crack propagation on sample.....	51
Figure 43	Recorded, a,P,d values.....	51
Figure 44	Excell table of P,a,d values.....	52
Figure 45	Calculation of Δ	53
Figure 46	Calculation of average G_{IC} values from 3 samples.....	53
Figure 47	GIC – a” graphs with average and standard deviations.....	54
Figure 48	Top view of flocked surface.....	54
Figure 49	SEM image of flocked prepreg.....	55
Figure 50	Angle measurement of flocks.....	55
Figure 51	Vertical alignment calculation table.....	56
Figure 52	SEM images of flocked surface.....	59

LIST OF TABLES

Table 1.	Effect of field application time on flock densities at different levels of constant voltage and distance.	27
Table 2.	Effect of voltage on flock densities at different levels of constant time and distance.	27
Table 3	Effect of flight distance on flock densities at constant voltage and different levels of constant time.	27
Table 4	GIC values of 0.4mm N66 flock used laminates(N66).	37
Table 5	GIC values of silane treated 0.4mm N66 flock used laminates(N66-S).....	40
Table 6	Vertical alignment and density value of flocks	57

SYMBOLS AND ABBREVIATIONS

ASTM	American Society for Testing and Materials
CFRP	Carbon Fiber Reinforced Polymer Matrix Composites
DCB	Double Cantilever Beam
G_{IC}	Mod I Interlaminar Fracture Toughness
N66	Nylon 66
SEM	Scanning Electron Microscope
VA	Vertical Alignment

1. INTRODUCTION

The use of composite materials continues to expand rapidly. Composite materials were especially used in the defense industry, and recently have begun to take place in the structures of the automotive and marine industries. The use of composites in structural applications has been increased due to their higher specific strength, also known as stiffness to weight ratio [1-3]. At the same time, composite materials have properties that need to be improved due to possible damage modes. Delamination is a failure mode critically related to life of the composite structures among all other damage categories. It can be caused during manufacturing or by events such as large hailstones and bird strike events [4].

There are many methods to solve the delamination problem and they are based on improving the low interlayer (fracture) toughness in layered composites. Amongst these methods, the most efficient is making add-ons such as toughening particles, films, or fiber structures of different sizes [5]. These add-ons can be useful in increasing interlayer fracture toughness, but it brings volume and weight penalty to the composite structure [6]. To overcome this disadvantage, applications such as polymer-based electrospinning and electrostatic flocking are preferred instead of applications where metal materials such as z-pinning are used [7-9].

It is expected that add-on structures between layers will activate some toughening mechanisms during the delamination and exert effects that make crack progression difficult. The most effective of these mechanisms is the bridging mechanism [10]. In addition to electrospinning and z-pinning methods, electrostatic flocking is also used to activate the bridging mechanism [8, 11].

During the transition of additive fibers to inter-layer bridge positions, three different situations can occur (Figure 1). In the case of a strong interface with epoxy (i.e. in case of bonding), there would be no debonding trace in the failed interface and ductile fibers that have broken by thinning at the interface can be traced as an indicator of this case (Figure 1.b). If the interaction with epoxy resin is weak, the separated peeling would have the exact negative traces of fiber morphology on the surface, and a respective image would be formed (Figure 1.d). An intermediate of the two can occur if straining is possible after partial debonding (Figure 1.c) [12].

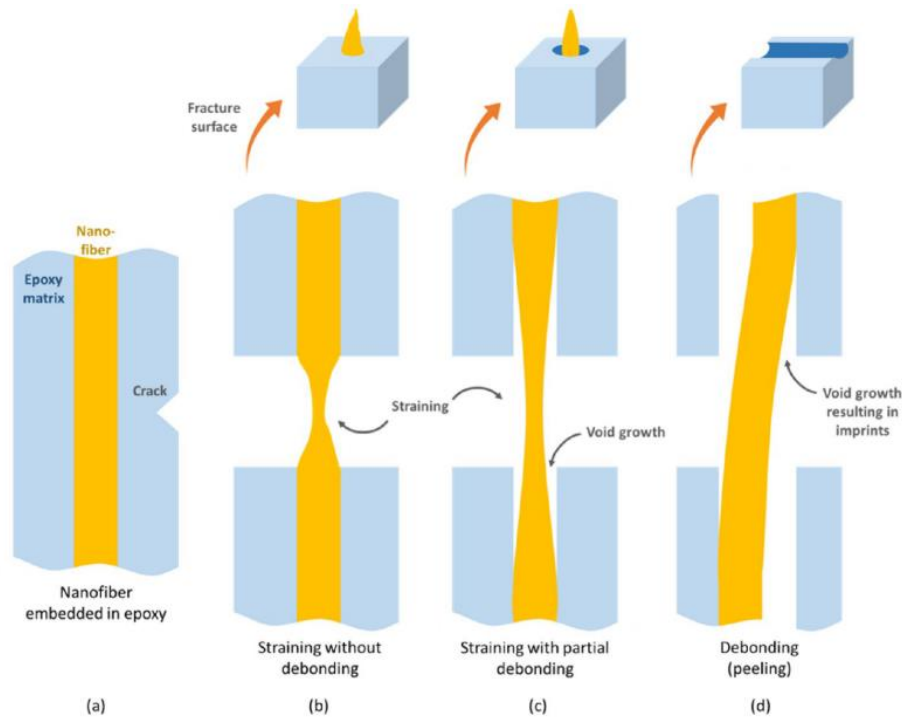


Figure 1 Interaction of a bridging fiber with the crack front. (a) Schematic view of an embedded fiber interacting with the crack front, which can result in (b) straining of the fiber without debonding, (c) straining of the nanofiber with partial debonding from the epoxy, or (d) complete debonding of the nanofiber (peeling). [12]

The z-pinning method is a very effective method to solve the delamination problem because the inserted rod is placed perpendicular to the direction of crack propagation, passing through all layers of the laminate [13]. The electrostatic flocking technique can be used to place small polymer fibers perpendicular to the crack propagation, as in the z-pinning method. Although the insertion angle of the modifier at the interface is similar, the electrostatic flocking method is different from the z-pinning method in that chopped polymer fibers (flocking) are placed on a single interface (between 2 layers) (Figure 2).

As an advanced application of the electrostatic flocking technique, studies have been carried out in which flocks are placed vertically at the composite interfaces. In these studies, it is known that brittle composite interfaces are toughened by using carbon fibers as well as nylon flocks used in the textile industry [7, 14]. In a study with 1.8 deniers, 1.3 mm long Nylon 6,6 (N66) flocks, which were placed on the surface in different amounts, it was shown that the fracture toughness increased by 1.5 to 3 times [7].

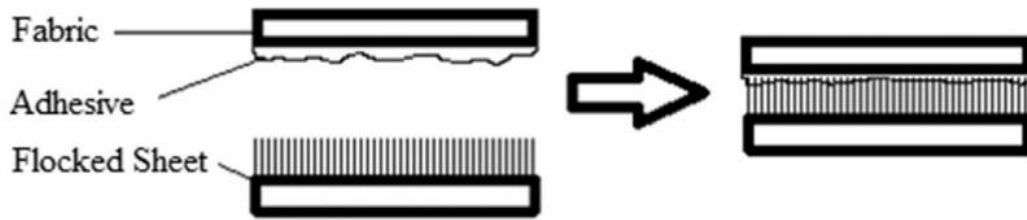


Figure 2 Schematic Diagram of Flocking Between 2 Layer [9].

From the studies in the literature, the positive effect of shortening the flock on the interface toughness is clearly seen [14]. While shortening of the flock becomes an advantage to operate the bridging method in interface toughening, it becomes difficult to place the short flocks exactly perpendicular to the surface [15]. However, the observations made until now do not show the limits of the effect of currently used industrial flocks on the interface toughness by electrostatic flocking. In this study, industrial flocking of N66 flocks with previously unused lengths (0.4 mm) was achieved on a carbon based prepreg. By placing these modified prepreg layers to mid-planes of the composites, the effect of flocks on the toughness of the interface was checked. The shortening of the length of the flocks was expected make it easier for the epoxy on the prepreg to be attached to its perpendicular ends. In addition, the use of flocks of similar size scale with the knit "hills and grooves" of epoxy-impregnated carbon fiber fabric could possibly increase the effectiveness of the flocks in the vertical bridge position.

In this study, the applied voltage and flight distance were optimized to place the N66 flocks vertically on the prepreg by experimental studies. In addition, the relationship between process parameters (flight time, voltage, distance) and flock density was examined.

It was determined that no surface modifications has been applied on the polymeric flocks with the purpose of improving the epoxy – flock chemical interaction until now. In this study, N66 flocks were treated with an amino silane molecule to provide a better interaction of the flocks with the epoxy surfaces due to the amine groups on them. The influence of N66 flocks and amino silane – treated N66 flocks on the interlaminar fracture toughness were compared.

2. LITERATURE SURVEY

2.1. Composite Materials

A new structure can be created by combining the desired properties of two or more monolithic materials. These combined structures are called hybrid materials. Composite materials are among the hybrid materials. Composites can be designed such that they can show superior characteristics compared to the individual components. The matrix and the reinforcement are generally the two constituents. Composite materials are characterized with their high strength and stiffness and low density. Reinforcement provides the much-needed strength and stiffness, and the matrix plays a crucial role in transferring the external loads to the reinforcement and forming the component with the desired geometry.

In general, types of fiber reinforcements used are continuous and discontinuous. Continuous-fiber composites usually have a desired orientation. Discontinuous fibers are on the other hand, oriented randomly. Chopped fibers and random mats are examples of discontinuous reinforcements and unidirectional, woven fabric, and helical winding are examples of continuous reinforcements. (Figure 3) [16]. Commercially available reinforcement fibers are aramid, carbon, polyester, fiberglass. The most common resins of the thermoset family and the ones mostly used in composite construction are polyester, vinyl ester, epoxy, and phenolic [17].

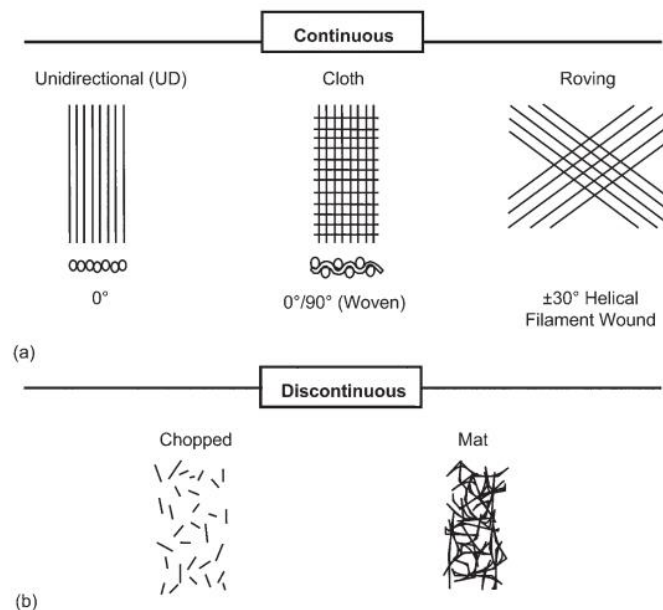


Figure 3 Typical reinforcement types [16].

The lay-up is called a lamina when there is a single-ply with all of the layers or plies stacked in the same orientation (Figure 4). The lay-up is called a laminate when the plies are placed at different angles. Continuous-fiber composites are often laminated materials in which the constituent layers, plies, or laminae are oriented in ways that improve the composites' resistance against the principal loads. [16].

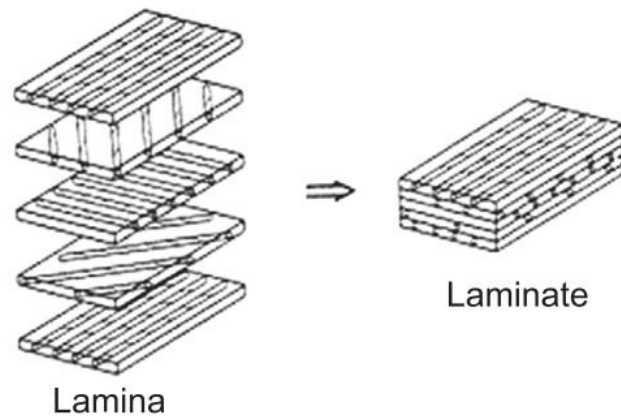


Figure 4 Lamina and Laminate lay-ups [3].

2.2. Composite Materials Damage Modes

Different damage mechanisms may occur in a carbon fiber reinforced polymer composite (CFRP). These mechanisms are given in Figure 5. The load transmission to the fiber is carried out through the matrix. The first damage mechanism (reinforcement fibers) occurs at the point where the fibers cannot withstand the load in in-plane stresses. Mechanisms 2 (fiber break) and 4 (fiber/matrix debonding) can occur when the load is carried by the matrix, not the fibers, under out-of-plane loads. Mechanism 3 (matrix cracking) depends on the strength of the bond between the matrix and the fiber, which in turn affects the mechanism of matrix – to – fiber load transfer. The 5th mechanism (delamination) is the most common damage mechanism observed in composite materials and causes a decrease in the fatigue life of the material [4, 18].

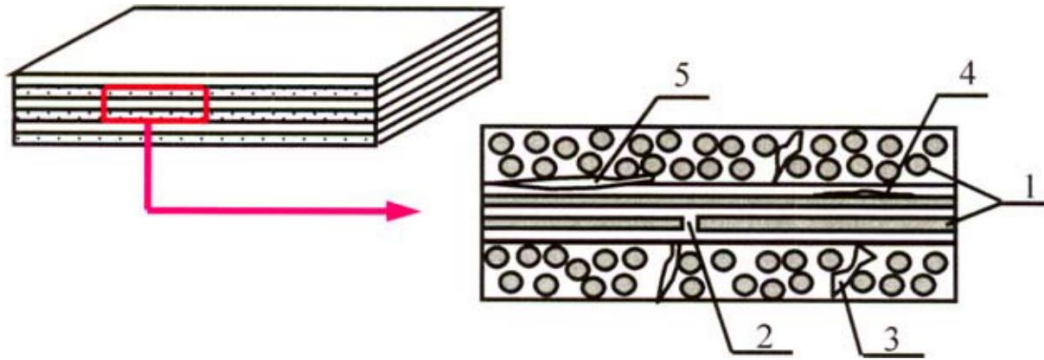


Figure 5 Schematic damage modes in CFRP laminate [6].

There are 3 main damage modes in the delamination mechanism. These are shown in Figure 6: (i) tensile mode (Mode I), (ii) shear mode (Mode II), and (iii) tear (twist) mode (Mode III). Crack opening or tensile mode of delamination is the most common form of fracture failure and named as Mode I. Here, the plies are pulled away from each other and as the crack propagates, the two new interfaces forming move away relative to one another [4]. The resistance of the CFRP material to crack initiation and propagation in these modes is called interlayer fracture toughness (G_{IC} for Mode I) and manifests itself as one of the mechanical properties of the material. Some test methods are used to determine this property of the material [8].

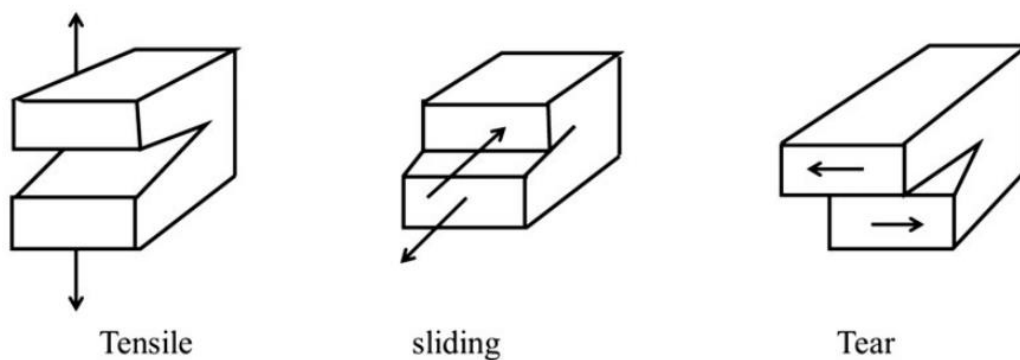


Figure 6 Various cracking modes for fracture toughness classification [4].

International standard organizations such as the European Structural Integrity Society (ESIS), the American Society for Testing and Materials (ASTM), Japan High Polymer Center (JHPC) prepare several test methods. Throughout this study, ASTM D 5528 –

“Method for Mode I Interlaminar Fracture Toughness of Unidirectional Fiber-Reinforced Polymer Matrix Composites” was used [19]. Using a double cantilever beam (DCB) sample cut out of a CFRP plate, one can calculate the Mode I interlayer fracture toughness (G_{IC}) using the method outlined in this standard.

Here, the DCB sample is a rectangular, constant-thickness composite material with a non-adhesive joint (insert) used to initiate cracks in the middle layer. The layer separation load is transferred to the sample through the piano hinge or loading block, as shown in Figure 7.

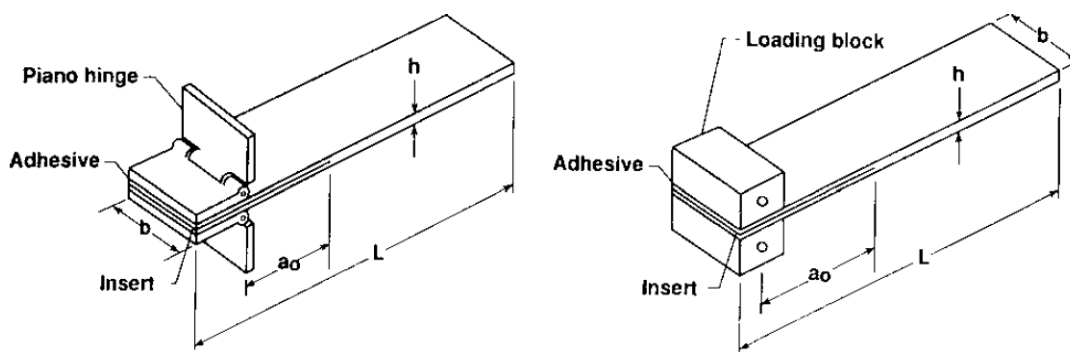


Figure 7 Double Cantilever Beam Specimen[19].

During the test, the load, and elongation values applied to the sample are recorded. Using these values, the G_{IC} value of Mode I interlaminar fracture toughness is calculated. Delamination starts from the non-adhesive insert placed in the middle layer and then increases and continues steadily in the DCB test. The G_{IC} value as a function of the crack length is plotted on the so-called Resistance Curve (Figure 8).

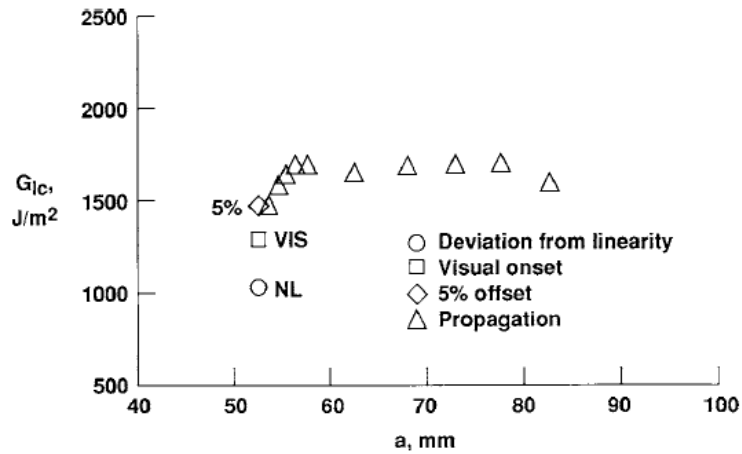


Figure 8 Delamination Resistance Curve (R Curve) from DCB Test [19].

VIS, NL, and 5% definitions are used to determine the G_{IC} initial values. VIS (visual) value is the values recorded at the first moment when the separation begins to be seen with the naked eye. The NL (nonlinearity) value is a point on the load-displacement graph where the behavior transitions from linear to nonlinear. For brittle matrices, these two values may be similar. The “5%” value is the value recorded at the cut-off point of the graph as a result of increasing the “slope⁻¹” value of the load-extension graph by 5%. The maximum load is considered if the transition occurs after the maximum load point. The G_{IC} value obtained by using NL is always smaller than other values and it is recommended to use this value for durability and damage tolerance analysis.

In order to measure the initial value and the progressive value of G_{IC} , before testing the DCB sample, a paint on both sides of the sample with a water-based pen is needed. After the insert layer, a thin pencil to draw the planned pre-crack lengths is used. Each 1 mm of the first 5 mm after the front crack is individually marked, and the next 45 mm is marked at 5 mm intervals. The load-displacement value is recorded when the sample reaches the crack area during the test. This can be done visually or with the help of a magnifying glass. In addition, another important point to be examined after the end of the test is whether the crack progression is parallel on both sides; if the difference between the locations of the crack on both surfaces is more than 2 mm, asymmetric loading may occur, and this issue should be evaluated.

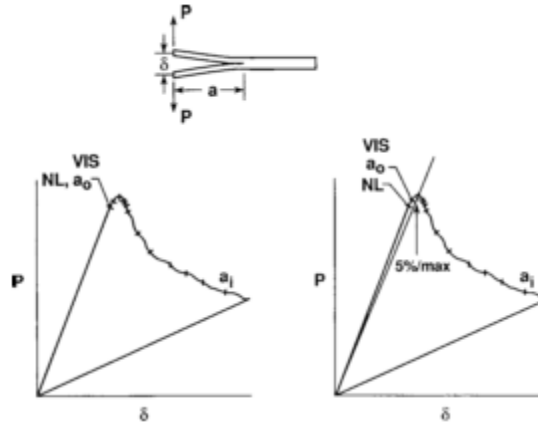


Figure 9 Load Displacement Trace from DCB Test [19].

After obtaining the load-elongation data recorded in Figure 9 at certain crack separation lengths by the method described above, the G_{IC} value for each separation length can be calculated. Modified Beam Theory is the method proposed by the ASTM standard and is a revised version of the 'beam theory'. The beam theory formula is as given as follows:

$$G_I = \frac{3P\delta}{2ba} \quad \text{Equation 1}$$

P = load

Δ = displacement (displacement)

b = sample width

a = length of layer separation (crack delamination)

The value of G_I calculated by beam theory is higher than it should be because it assumes that the DCB sample is perfectly prepared and there is no rotation during loading. So it needs to be corrected. Therefore, the instant separation length is greater than “a” and can be corrected with “a+ $|\Delta|$ ” and the formula is revised as follows:

$$G_I = \frac{3P\delta}{2b(a + |\Delta|)} \quad \text{Equation 2}$$

To obtain the Δ value, the 'compliance' C value is used. C is equal to δ/P . In the graph where the C1/3 value is plotted against the layer separation lengths, the point where the graph cuts the x-axis (Figure 10) gives the Δ value.

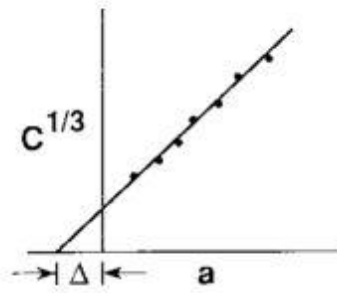


Figure 10 Modified Beam Theory [19].

2.3. Methods to Increase Delamination Resistance

There are many methods to solve the low interlayer toughness and related delamination problems; adding toughening particles, films, chopped fibers(flocks) or fiber structures of different sizes. In addition to adding materials to the interfaces of laminates, 3D knitting of fibers or z-pinning methods are also used [4].

Byung Chul Kim et al. placed differently sized thermoplastic N6 and N12 particles in the middle layers of the prepregs. They observed that the reduction of interface toughness occurs when polymers of different sizes do not interact well with epoxy. Likewise, while emphasizing the positive effect of shrinking particles on the interface toughness, they observed that the difference between the curing temperature and the melting temperature of thermoplastics is an important parameter [20].

Yiping Qiu, et al. increased the delamination resistance using poly (phenylene oxide) (PPO) particles. DCB and ENF tests were applied to examine the effect of PPO particle size on Mode I-II interlaminar fractures. When 10 wt% of PPO particles are placed with a particle size ranging from 10 to 50 microns, they achieved a 65% increase in mode I and a 40% increase in mode II [21].

Coating (functionalizing) carbon fibers used in CFRP with various chemicals or structures is a method for improving the mechanical properties of the composite. In an example, Sager investigated the effect of this method on the mechanical properties of carbon nanotubes coated carbon-fiber-reinforced epoxy-based composites. While the coating of the fibers caused a decrease in the tensile properties of the composite, it increased the shear resistance between the layers [22].

As an example of a study, in which the reinforcement in the matrix was functionalized, Pinto et al. examined silane-treated jute epoxy composites. The impact of surface treatment on the interlaminar fracture and delamination resistance of jute fiber/epoxy laminate composites was investigated in this work. Alkali scouring followed by silane grafting enhanced the interfacial bond strength and improved delamination resistance of jute/epoxy composites by 10% [23].

In some applications, the reinforcing material in the composite material is processed, and the functionalized particles are added to the interface to increase the delamination resistance. One of these application examples can be seen in the work of A. K. Lau *et al.* Braided carbon/epoxy and carbon-CNT/epoxy composites were fabricated after modifying the multi-walled carbon nanotubes (MWCNT) with acid or silane. Silane treatment resulted in superior flexural modulus (by 10%), strength (15%) and wear properties, compared to acid treatment. Improvements were correlated with the improved quality of dispersion that was achieved with the silanization of the MWCNTs [24].

Another method to increase fracture toughness is to place functionalized thermoplastic veils at the interface. Previously, our research team studied use of thermoplastic blends in veil form as a novel strategy which had previously been examined by using electrospun fibers of homopolymers as well as their physical mixtures. While separate toughening mechanisms were activated by the individual presence of the physically mixed fibers in the previous studies, it was shown that it is possible to initiate a concerted action of these mechanisms by interleaving electrospun fiber veils based on blends of PCL and PA6 (80/20, 60/40 and 40/60). Phase separation tendencies in the fibrous blends activated different toughening mechanisms simultaneously. Fiber debonding from the epoxy matrix resulted in unobstructed peeling of PA6 interleaved layers in mode I; whereas PCL toughened the interfaces by plasticizing the epoxy. Debonding followed by an effective bridging along the strong axes of fibers was only possible at a certain level of phase separation that permitted penetration of PCL into the epoxy matrix and allowed these regions to function as “bridge pillars” upon melting during curing. Increase in G_{IC-ini} value was highest in the 60/40 blend; 69% compared to unmodified interface. [8]

Saghafi et al. investigated the effects of systems on the delamination behavior of composites where PCL and N66 are used individually and in layers. In that study, veils produced were placed between unidirectional glass fiber reinforced epoxy prepreg layers and curing was carried out in an autoclave (pressure not specified, 150 °C) in a vacuum

bag. There is no clear information about the amount of polymer placed between the layers. N66, PCL, and N66/PCL laminated fiber blends showed an average increase in G_{IC} of 4.5%, 25%, and 21%, respectively. In addition, it was concluded that N66 and PCL polymers had the opposite effect of each other in the G_{IC} initiation and G_{IC} progression stages, and it was shown that the mixture of both polymers was effective in both stages. In the G_{IIC} tests conducted in the same study, it was observed that N66 was more efficacious than PCL in the direction of Mode II, and the mixture increased by 56% in total in the G_{IIC} value. After the observations made on the fracture surfaces, it was interpreted that PCL fibers melted during curing and stood in a second phase as a result of phase separation in the matrix, while N66 fibers preserved their structures [25].

Delamination resistance can also be improved via through-thickness methods such as Z-pinning and 3D braiding. In the application of these two methods, modifications are not made to a single interface but they are applied to all layers.

V. Ranatunga studied the effect of carbon rods against delamination through the z-pinning method. Also compared was the z-pinning with flocking application, in which 1.8 deniers, 1.3 mm long Nylon 6.6 flocks were used. Z-pins were inserted to the half bottom layers of composites and G_{IC} was improved by 13 fold. By applying flocks of varying densities on the interface, 1.5 to 3-fold increase in G_{IC} value was achieved. Z-pinning was not effective in increasing Mode-II non-precracked fracture toughness (NPC), although it did enhance the precracked toughness (PC) by around 28%. Flocking with a lower areal density increased the NPC by 80% and PC by 126%, whereas high density increased the NPC and PC by around 51% and 74%, respectively [7].

J. Rice *et al.* studied 3D woven and through-thickness reinforced laminar composites. Impact of braiding angle and yarn size on fracture toughness were investigated in 3D wovens along with other parameters. Fracture toughness increased as the number of filaments increased, contrary to the opposite trend observed with the braiding angle. Although improvements with flocking (8-9 fold) were less than those with 3D braiding (10-12 fold), the 3D braiding method, was noted as having a serious drawback time-wise in the design and fabrication stages. Flocking on the other hand, was expected to enable use of various sample geometries with lower application time and cost [26].

J. Rice *et al.* stated that the electrostatic flocking method is cheaper and faster compared to other z-direction strengthening studies. Although it has less impact on G_{IC} than other

applications, low cost and high speed makes the electrostatic flocking method more desirable. In addition to being fast, electrostatic flocking is one step ahead of z-pinning and 3D weaving applications with low weight penalty.

The flocks placed at the interface with the electrostatic flocking method are similar to the methods of adding particles or films to the interface in terms of the weight penalty. But it is similar to the z-pinning method in terms of placing the flocks perpendicular to the surface. While the rods added in the z-pinning method are placed through all layers, the placement of the flocks on a single interface differs from the z-pinning method.

2.4. Electrostatic Flocking

Sticking of particles to an adhesive-coated surface under the effect of a field is known as flocking. Generally, finely chopped natural or synthetic fibers are used in flocking applications. Flocked surfaces can both be decorative and functional. The electrostatic flocking method is the most ideal flocking method for positioning short fibers perpendicular to the surface [27]. Among these methods, the most ideal flocking method for positioning short fibers perpendicular to the surface is electrostatic flocking. These short fibers are called flock. In the textile industry, different polymers are used as flock. Polyester, polyamide, rayon cotton, acrylic are among these flocks [28]. In mass production in the textile industry, it is preferred that the flocks are placed as vertically as possible and that the surface to be coated is covered with the maximum number of flocks. Although the starting point is the textile industry, it is also applied in decoration, paint and even automotive sectors [28].

Electrostatic flocking process, using a DC electric supply, is shown in Figure 11. The rotating brushes in the upper part, mix the flocks and press the grid-shaped electrode. The grid-shaped electrode is charged with negative DC high voltage. During the contact, the outer surface is conductive, and the semiconductor flock is negatively charged. Negatively charged flocks travel along electric field between the grid and the grounded sub-surface. The cylindrical flocks come to a vertical position along the electric field and adhere vertically to the glued surface at the bottom [28].

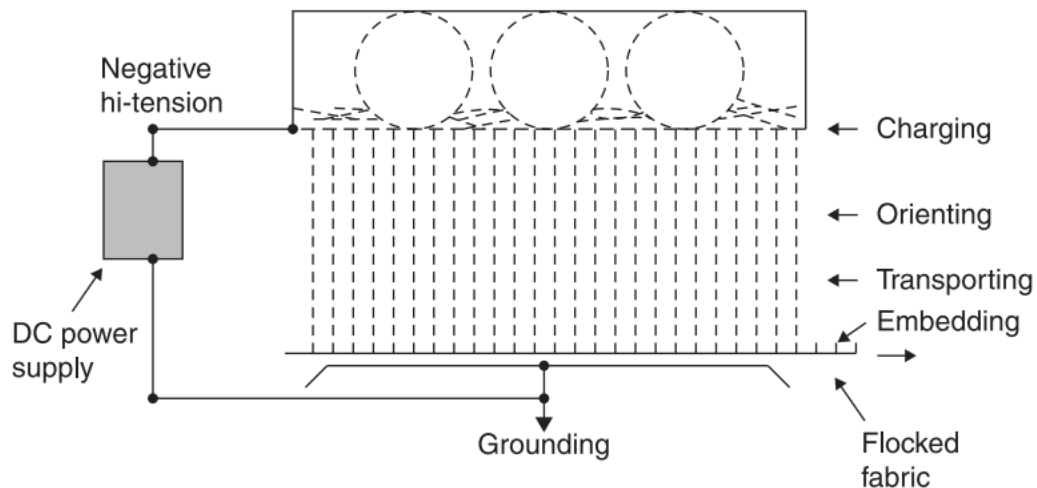


Figure 11 DC Flocking Process [28] .

Apart from the process described above, there are also new flocks and developing application areas. In the field of tissue engineering, chitosan flocks produced using the cutting method have been transformed into a bioactive scaffold. It has also been proposed to use carbon fiber flocks produced by the cutting method in the production of innovative thermal interface materials. In addition, in some studies using polyamide, polyester, carbon fiber, and carbon nanotube as flock, it has been shown that the interface toughness of glass fiber and carbon fiber composites can be increased [29-35].

With advanced applications, it has become important to place the flocks more perpendicular to the surfaces. There are some studies about placing the flocks more perpendicular to the surface. In the study of placing carbon fibers on the surface by electrostatic flocking, the holding angles of 0.5-1-2 mm carbon fibers to the surface under the same conditions were studied. In that study, it was observed that N66 and carbon fibers with a length of 1 and 2 mm can be placed more vertically than fibers with a length of 0.5 mm. To examine the effect of applied voltage, different magnitudes of voltage (10, 20, 30 kV) were applied. It was observed that carbon fibers were placed more vertical (55% of population) under 20 kV (Figure 12). They concluded that a proper panel distance and voltage was needed to make sure the fibers have enough time to be rotated along the electric field direction [29].

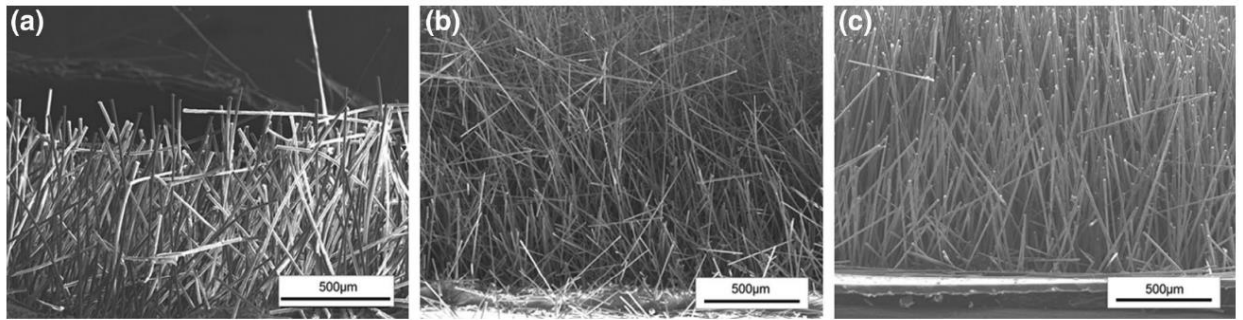


Figure 12 Arrangement of (a) N66 fibers, (b) PCFs (PAN-based carbon fiber) and (c) mPCFs (mesophase pitch-based carbon fibers) after electrostatic flocking [29].

Flock density was also studied in the work of S. Yang et al. for the production of neatly cut short polyamide flocks (so-called superfine flocks). The effects of application distance, voltage, and time on the fiber density on the surface were observed. Since these variables cannot be evaluated in isolation, in a series of experiments the optimal conditions of placing 0.2 mm polyamide flocks densely were studied. The optimal process parameters were experimentally determined as 7 cm, 60 kV and 10 secs [15].

In composite applications, flocks can be placed at the interface of each layer or the required number of composite layers. This can also allow interfacial toughness improvements to be combined with other improvements, like in design of energy-absorbing materials.

For example, Pinto et al. researched the mechanical properties of silane-enhanced jute epoxy composite structures using 3-denier, 1.3 mm length nylon flocks besides other flocs. The delamination resistances were enhanced by 81% and 65%, for the plain weave and unidirectional composites, respectively. ILSS of the same composite variations showed an increase of 13% and 16%, respectively. The in-plane tensile characteristics were reduced for both variations. This may have been due to the excessive increase in the overall thickness of the final laminates, although this was not discussed in detail, in the manuscript. On the hand, the decrease in the in-plane properties with the modification of each layer of the composite with flocks, calls for a careful control on the areal density and sizes of the flocks, that are intended to be utilized for similar purposes [23].

Armand F Lewis et al. studied energy-absorbing materials produced by flocking (FEAM). The energy loss values upon impact were measured using a ball drop test. Several parametric studies were conducted to identify the best flock type (PET or Nylon) and size

for FEAM. In a specific FEAM configuration (2 mm – 20 denier double-side flocked nylon), it was found that constructing FEAMs with multi-layer two-side flocked fabrics and using a divider sheet between them to prevent the flocks from intermeshing with each other during curing is important [9].

Y.K. Kim, A. F. Lewis, et al. composed their work on composite materials with electrostatic flocking. In general, different sizes and types of flocks were applied to glass fiber composites. The effects of this on the interface toughness were examined. Within the scope of the study, Mode I fracture toughness of glass fabrics with epoxy matrix was studied using 3 deniers, 2 mm long nylon flock, 3 denier, 0.6 mm long polyester flocks. In this study, electrostatic flocking was applied with 3 different methods; i) wet flocking, ii) dry flocking and iii) pre-flocking. In general, these applications differ from each other by the differences in the applying stages of the epoxy used as the adhesive with the fabric. In the wet flocking study, fracture toughness improved by 8 times by using 3 denier, 2.0 mm long nylon flocking. In dry flocking, they observed that using 15 deniers, 3.8 mm long nylon flocking, the fracture toughness increased by 82%. In pre-flocking method, fracture toughness improved by 3.2 times by using 3 denier, 1.2 mm long nylon flocks.

A significant increase has been achieved in wet flocking and pre-flocking methods. Since epoxy is applied manually just before flocking in the wet flocking method, it is doubtful that the homogeneity of the amount of epoxy on the interface can be repeated. In the pre-flocking method, epoxy impregnated prepregs are used directly. With the amount of epoxy at the prepreg interface measurable and controllable, it will be a better reference for comparisons in the flocking study.

There are studies on the vertical placement of flocks on water-based adhesives in industrial flocking. Parametric studies have not been performed for prepregs, which have a much different conductivity than water-based glues and have charge accumulation on them. The potential charge accumulation problems on the prepreg surfaces will be important to consider in vertical alignment of flocks.

Previous studies also show that when the flock lengths used got smaller, the mode I fracture toughness values tended to increase. However, for the purpose of increasing the interface toughness, the shortest flocks used have been 1.3 mm long N66 and 0.6 mm long polyester flocks, until now. Apart from these studies, it was also observed that the electromechanical properties of the carbon fiber flocks get better as the lengths of the

flocks get shorter [36]. It is predicted that the interface toughness of layered composites could be increased by using the shortest commercially available flocks. Considering also that the applied flocking density would be critical in allowing the penetration of epoxy resin, in this study the interlaminar toughness of composites were tried to be improved with commercially available shorter N66 flocks and their amino silane-treated versions.

3. EXPERIMENTAL STUDIES

3.1. Materials

3.1.1 Flocks

Flocks were supplied from Flokcan Textile (Turkey). Mainly three different types of N66 flocks were used throughout the study; (i) 2 mm long black paint coated flocks, (ii) black colored 0.6 mm long 1.7 dtex flocks that are used commercially and (iii) 0.4 mm long 0.9 dtex flocks that were prepared specifically for this work by the producer. It was stated by the producer that the commercial black flocks were coated both with a dispersant and a conductive agent; while the 0.4 mm flocks had to be coated with the dispersant for production necessities, but not necessarily with the conductive agent as per our request. Obtaining pristine flocks for ensuring a defined “interlayer epoxy – flock interaction” was a priority in this study. This was achieved to a certain extent with the exception of mandatory “dispersant” and can be considered as one of the limitations of this work.

3.1.2 Surface Treatment of Flocks

For testing the efficacy of a surface treatment of the flocks prior flocking operation, to possibly increase the interaction of flock surfaces with epoxy during curing; a set of flocks were treated with a silane. APTES (3-aminopropyl)trimethoxysilane) (97%) was purchased from Alfa Aesar and used for this purpose.

Before making silane treatment on N66 flocks, the surfaces had to be cleaned and activated. In the experiment, 0.4 mm N66 flocks were treated with oxygen plasma for 15 minutes. After the oxygen plasma, the hydroxyl groups are formed at the surface of the N66 flocks. After plasma treatment, flocks were taken out and placed in vacuum desiccators. APTES was added to the desiccator medium in a small container. Then, vacuum was applied to desiccator. At room temperature, the APTES molecule passes into the gas phase under vacuum. Under these conditions, silanes first hydrolyze and release methanol, then hydroxyl terminated silane molecules form hydrogen bonds with hydroxyl groups on the surface of the flocks. Finally, a condensation reaction at the surface yields covalent functionalization of the surface with amine groups. The purpose of this modification is to enhance the adhesion between N66 and epoxy resin as the resin is expected to react with amino-functionalized flocks in the same way as it reacts with its hardener (Figure 13).

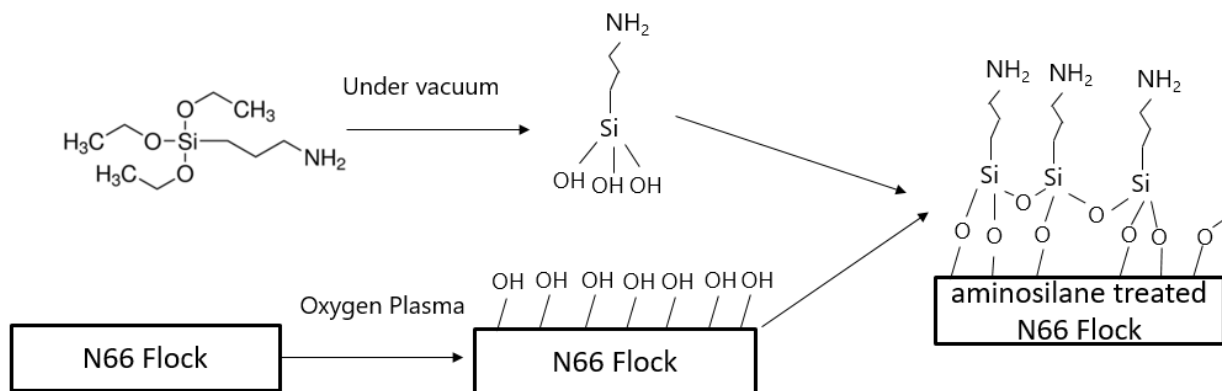


Figure 13 Aminosilane treatment.

3.1.3 Prepreg

Carbon fiber prepreg (VTP H 300 CFAT 200 3 KT RC 42 HS) was purchased from SPM Composites and Advanced Material Technologies Inc. Prepregs were composed of 2x2 twill carbon fiber fabrics with 200 g/m² areal density and 42 wt% epoxy resin.

3.2. Electrostatic Flocking Application Cabin

In order to understand the mechanism of the electrostatic flocking technique as it is applied in the textile industry, a commercially used flocking cabin was purchased from Elektrosis Machine (MPW2000 Flock Printing). In these preliminary trials, commercially used decorative and conductive flocks (2 mm long black paint coated N66) were used. In the cabin given in Figure 14, flocks were placed on the metal bottom plate that was grounded and a positive static voltage was applied to the grid between the target and flock plates for a determined time. The position of the grid was adjusted with the hoses on the side walls of the cabin, but the hoses originally supplied were not stiff enough to maintain the parallelism between the grid and the top plate. A regular white paper coated with water-based conductive adhesive was used as the target surface. A metal plate which was also grounded through the power supply was placed on the back of the target to ensure the continuous movement of the flocks through the electric field after passing through the grid. The results of these studies were evaluated qualitatively and will not be reported here.



Figure 14 Commercial electrostatic flocking cabin.

3.3. Flocking Setup for Interfacial Engineering of Layered Composites

In textile applications, the flock density on the surface is desired to be high to create a velvet like surface. Conversely, for interlayer modifications, the flock density should be such that it should not hinder the flow of the epoxy between the composite layers during curing. Therefore, the flock density on the surface was presumed to be an important parameter. This necessitated some modifications to the initial setup.

The flock and target plate areas of the initial setup were larger than what is generally needed in the interlaminar toughness test specimen preparations. Therefore, for practical purposes (i.e., easy cleaning, proper prepreg handling before clean room...etc.), an additional internal cabin which would be positioned in the main cabin was produced. In order to ensure the linearity of the electric field lines while transporting the flocks, plexiglas was used in construction of this internal cabin, as well. Except the flock exposed surfaces of flock plate and the grid, all circuit connection wires were isolated with polyethylene tubing or shielded on the backside of the target plate. It is important that the grid and the top plate are parallel to each other in order for the flock density to be homogeneous on the target prepreg surface. A rack system that would allow the easy adjustment of the distances between the grid, flock plate and the target was configured on the walls of the internal cabin (Figure 15).

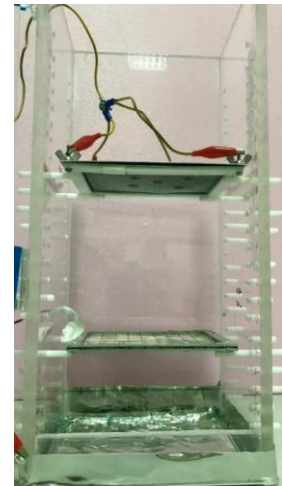
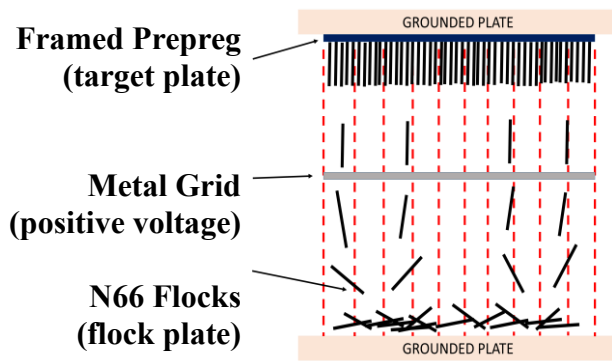


Figure 15 Designed flock cabin.

The way flocks were positioned on the surface (i.e., their areal density and vertical alignment) was analyzed by varying the applied voltage to the grid and the distances between the plates and the grid. Different magnitudes of electric field intensities (voltage/total distance, kV/cm) were obtained by changing these two variables. While the grid dimensions were taken down to 140×110 mm, the framed target that held the prepreg structure, which is given in Figure 3, consisted of 4 layers: (i) A metal back plate to create a uniform electric field between the grid and the target, (ii) prepreg surface that is to be flocked, (iii) a secondary metal frame to obtain a better grounding through the the carbon fibers of the prepreg and shortening the discharge time of the flocks over the low conductivity epoxy, (iv) a plexiglass cover frame to minimize the disturbing effects of the exposed metal frame on the electric field.

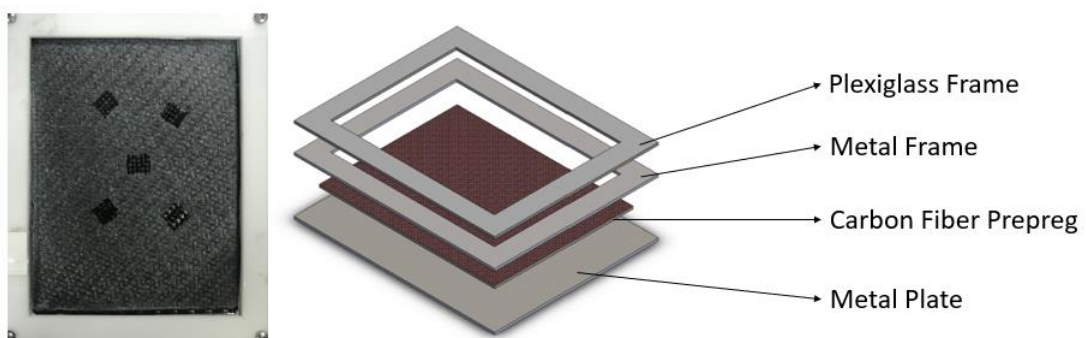


Figure 16 Frame for prepreg.

3.4. Lay-up Process

140×110 mm rectangular prepregs were cut from the prepreg fabric roll in a clean room environment. Prepregs were arranged in the 8-1-9 configuration for preparing the DCB test samples. Flocks were placed on the single layer that forms the mid-plane before its assembly with the bundled layers.

Two different non-adhesive films were used to initiate the delamination on the modified mid-plane of the laminates. In previous studies of our research group, 6-7 lines of 12 mm wide 75 μm thick Teflon tapes were used. However, while positioning them in the currently adapted configuration of the DCB test specimens, these tapes were frequently slipping and epoxy leakages along the initial crack were observed. To prevent this leakage problem, after some progress in the experiments, 55 μm thick continuous polyester films (Tesaband) were preferred instead of the initially used Teflon tape. The effect of this change will be discussed in the results section. Non- adhesive tapes or continuous films were laid along the first 62.5 mm of the 9-layer stack (Figure 17).

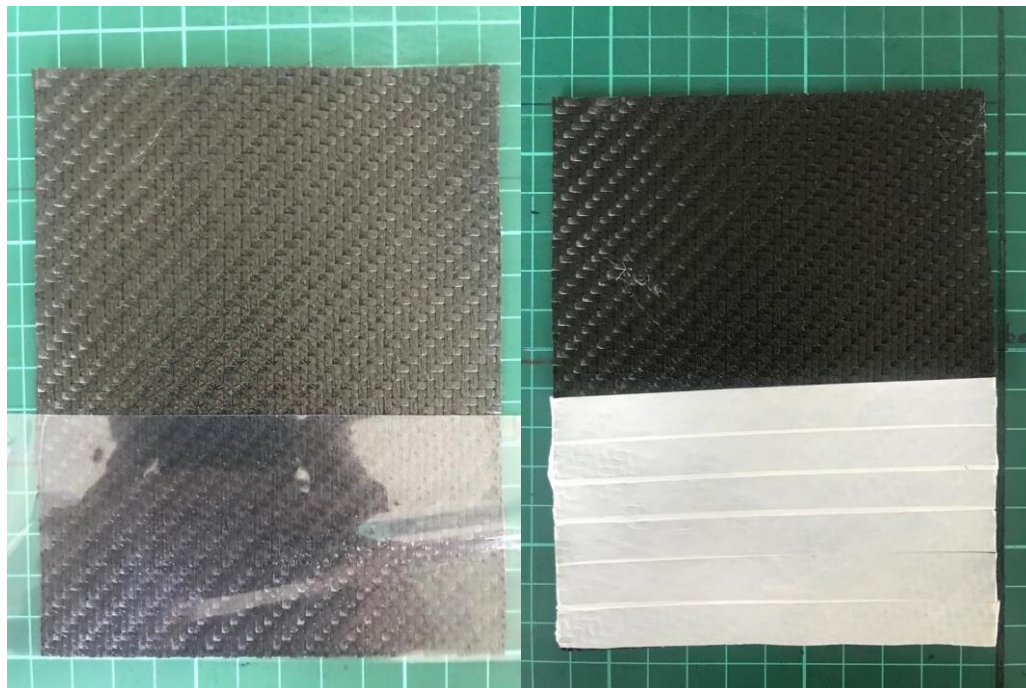


Figure 17 Teflon band and continuous film laid prepregs (9 layer side).

After combining the flocked single layer prepreg with the 8-layer bundle a second 9-layer stack was obtained. The composite with 18 layers was obtained by covering the first stack (i.e. non-adhesive laid 9-layer stack) over the second. This assembly was cured with the thermal cycle presented in Figure 18.

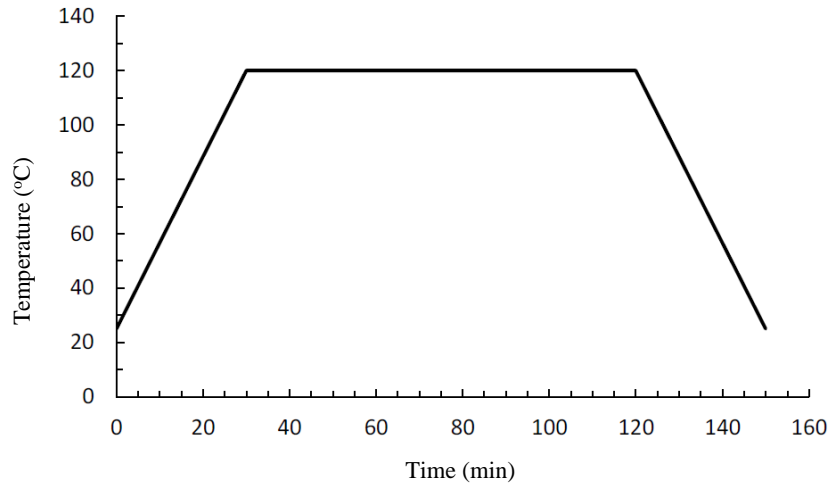


Figure 18 Curing cycle.

The curing process was carried out in a hot press that was furnished with heaters inside the two aluminum molds. Temperature was controlled with a PLC controller (Gemo TT109). During the curing cycle, a pressure of 7 atm. was applied on the assembly and continuously compensated manually. The cured composite was cut with a circular diamond saw that was operated at 13,000 rpm to produce the three 26×120 mm and five 7.4×14.8 mm test coupons for the ASTM 5528 and ASTM 2344 tests, respectively.

3.5. Mechanical Test for Mode I Fracture Toughness

DCB test coupons tested according to the ASTM 5528 standard for determining the Mode I fracture toughness of the composites. Each coupon was attached to the testing rig (Baz Makina) with the custom made to the loading blocks (Figure 19). A load cell (Keli) with a capacity of 1 kN was used during the tests and the tests were carried out at a speed of 1 mm/min. A video camera (Logitech – HD Pro C920) was used for crack tracking. Load and displacement values were recorded during the test once the crack hit the predetermined length. Mode I fracture toughness value (G_{Ic}) was calculated using these

values according to the method described in Section 2.4. Further details of the test and the specimen are given in Appendix 1.

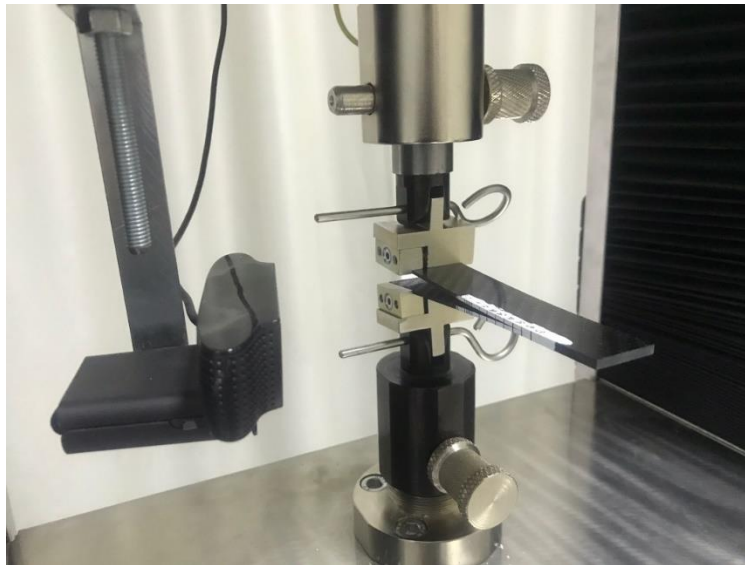


Figure 19 Test coupon placed in mechanical test machine and camera used for crack capturing.

3.6. Material Characterization

3.6.1 Scanning Electron Microscope (SEM)

Although the sizes of flocks used were large enough to view them under an optical microscope, an SEM (FEI Quanta 200F) was used because clear imaging could not be collected with the depth of field and contrast settings of the optical microscope. To prepare the samples for SEM investigations, 10×10 mm cut prepregs were placed on the main prepreg surface to be flocked as shown in Figure 20. After the flocking process, these small pieces of prepregs were peeled-off from the surface and their surfaces were examined for determining the flock densities and vertical alignments of the flocks under certain flocking conditions. ImageJ program was used for quantifying these observations and the details of the procedure are given Appendix 2. DCB coupons were cut with a metal guillotine after the test was finalized. Mid-layer cleanliness was preserved by adhering the failed crack tips with a tape before the sampling. The delaminated surfaces were examined with SEM to determine the interleaving efficiency and activated toughening mechanisms.

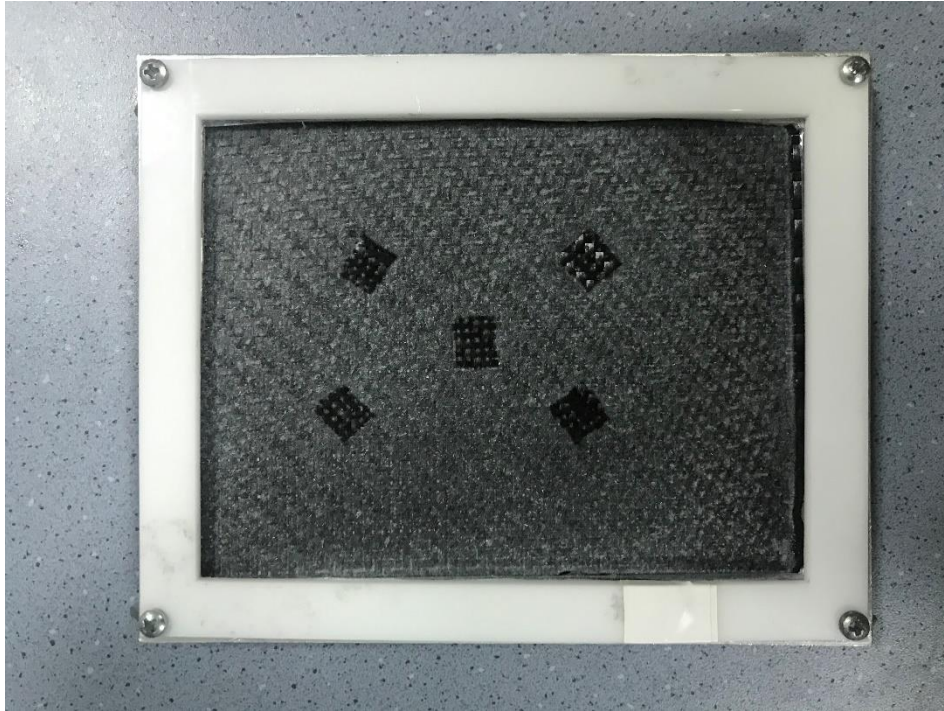


Figure 20 Framed carbon fiber prepreg with SEM coupon positions on it.

3.6.2 Fourier-Transform Infrared Spectroscopy (FT-IR)

An attenuated total reflectance (ATR) accessory was used to record the FT-IR spectra of the samples (PerkinElmer – UATR Two, METU Chemical Engineering Department). Each spectrum collected was the average of 64 scans in the $500 - 4000 \text{ cm}^{-1}$ range and they were collected with 4 cm^{-1} resolution. FT-IR analyses was used to examine the efficacy of the silane treatment steps.

4. RESULTS AND DISCUSSION

4.1. Electrostatic Flocking Studies

Flocking process can be controlled by considering mainly the effect of three process parameters, namely; voltage, distance and field application time. These three parameters have certain effects on vertical alignment of the flocks and flock density (flocks/mm²) on surface. The possible effects of these parameters on alignment and density were already mentioned in the respective part of the literature survey. Voltage to distance ratio can be another guideline in understanding and quantifying the effect of “electrical field” on the flocks. It should be noted that similar electrical fields can be acted on the flocks by simultaneously changing both the voltage and distance. It is also important to note that with the setup configuration used in this study, it was possible to change the distance between the flock plate and the grid (Y) or the grid and the target plate (X) or the two grounded plates (X+Y) (Figure 21). Therefore, without changing the field intensity, it was possible to study the effects of travel distances between different sections of the flock trajectory.

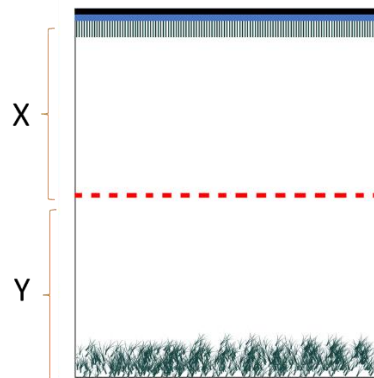


Figure 21 Illustration of setup, X: distance between grid and top plate, Y: distance between the grid and bottom plate

4.1.1. Controlling the Areal Density of 0.6 mm 1.7 dtex N66 Flocks

Effect of the three process parameters on flock densities on epoxy resin prepregs were examined first with black colored 0.6 mm N66 flocks. Areal density changes with each of the parameters are summarized separately in Tables 1-3. In the experiments conducted for understanding effects of field application time and voltage, although total flight distances were kept the same (i.e. 410 mm), X and Y were varied.

Table 1 Effect of field application time on flock densities at different levels of constant voltage and distance.

Y (mm)	X (mm)	Voltage (kV)	Time (secs)	Density (flock/mm²)
200	210	50	3	11
200	210	50	10	22
200	210	50	15	37
150	260	80	3	26
150	260	80	5	71
200	210	80	3	63
200	210	80	5	86
200	210	80	10	93
200	210	80	15	107

Table 2 Effect of voltage on flock densities at different levels of constant time and distance.

Y (mm)	X (mm)	Voltage (kV)	Time (secs)	Density (flock/mm²)
150	260	50	5	49
150	260	80	5	71
200	210	50	3	11
200	210	80	3	63
200	210	50	10	22
200	210	80	10	93
200	210	50	15	37
200	210	80	15	107

Table 3 Effect of flight distance on flock densities at constant voltage and different levels of constant time.

Y/X	Y (mm)	X (mm)	Voltage (kV)	Time (sn)	Density (flock/mm²)
0.58	150	260	80	3	26
0.95	200	210	80	3	63
0.58	150	260	80	5	71
0.95	200	210	80	5	86

It was observed that both the field application time and voltage are directly proportional to the areal flock densities on the surface at this fixed total distance of 410 mm (X+Y),

regardless of the ratio of Y and X (i.e. Y/X). When the distance between the top and bottom plates ($X+Y$), time and voltage were kept constant and the grid moved away from the lower plate (i.e. approaching the upper plate or equivalently increasing Y/X from 0.58 to 0.95), areal flock densities on the surface increased, increase being less pronounced at longer field application times (3 versus 5 seconds).

4.1.2. Controlling the Areal Density of 0.4 mm 0.9 dtex N66 Flocks

In Figure 22 the changes observed in flock densities and vertical alignment with the electric field were summarized in the same graph. It is interesting to note that when electric fields of similar magnitudes (around 2 – 2.4 kV/cm) were applied, the density and vertical alignment (VA) (percentage of population) of the flocks on the surface can take on different values. One of the primary factors that leads to this seemingly puzzling result is the fact that it takes a while for the flocks to be electrostatically charged and then rotate to the vertical position in the time, while travelling from the lower plate to the upper plate after lift-off. However, in all these series of experiments flight time was kept constant. Evidently, the other possible factor is the fact that similar electrical fields can be imposed on the flocks by changing the voltage and total distance together. If the same data was replotted for only the experiments with same levels of applied voltage, but different distance between the top and bottom plates ($X+Y$), a better insight to the effect of flocking parameters can be obtained. In Figure 23, the density and VA of flocks are given with respect to ($X+Y$), where Y was kept constant, but X was varied. Y was kept constant to understand the effect of elimination of variable grid exit velocities on the VA and density. The density increased almost linearly with increasing X, while the VA value increased up to a certain point and then decreased. The flight time of some the flocks to reach the top plate, which are exposed to less electrical force with increasing X, can be predicted to increase under the electrical forces that are getting smaller. The increase in relative flight time for some of the flocks can allow the flocks reaching the top plate initially to be discharged, before the charged flocks that are yet to reach the surface. Thus, charge accumulation on the surface is predicted to be rather auto-regulated as X is increased. The reduction of charge accumulation on the surface can allow more flocks to be placed on the surface and hence lead to an increase in the areal density. Increasing the X beyond a limit probably caused a drop in the electric field and the absolute electrical force and charge on the flocks which might have affected the VA adversely (Figure 23).

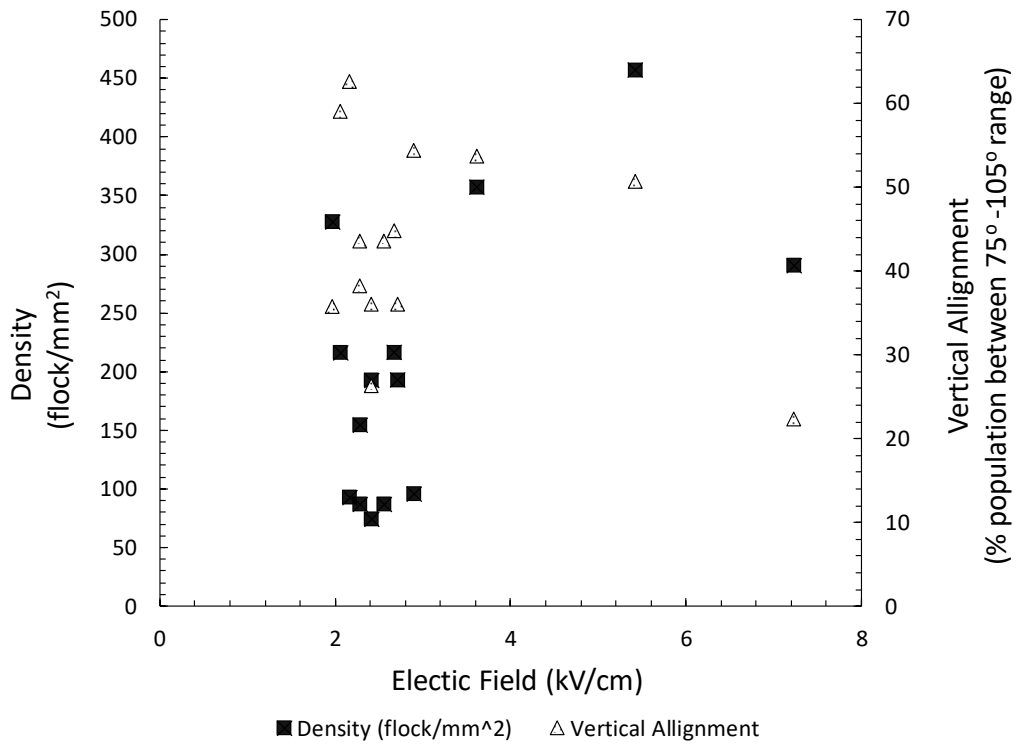


Figure 22 VA and areal density changes with respect to electric field for 0.4 mm N66 flocks (time is constant in all experiments).

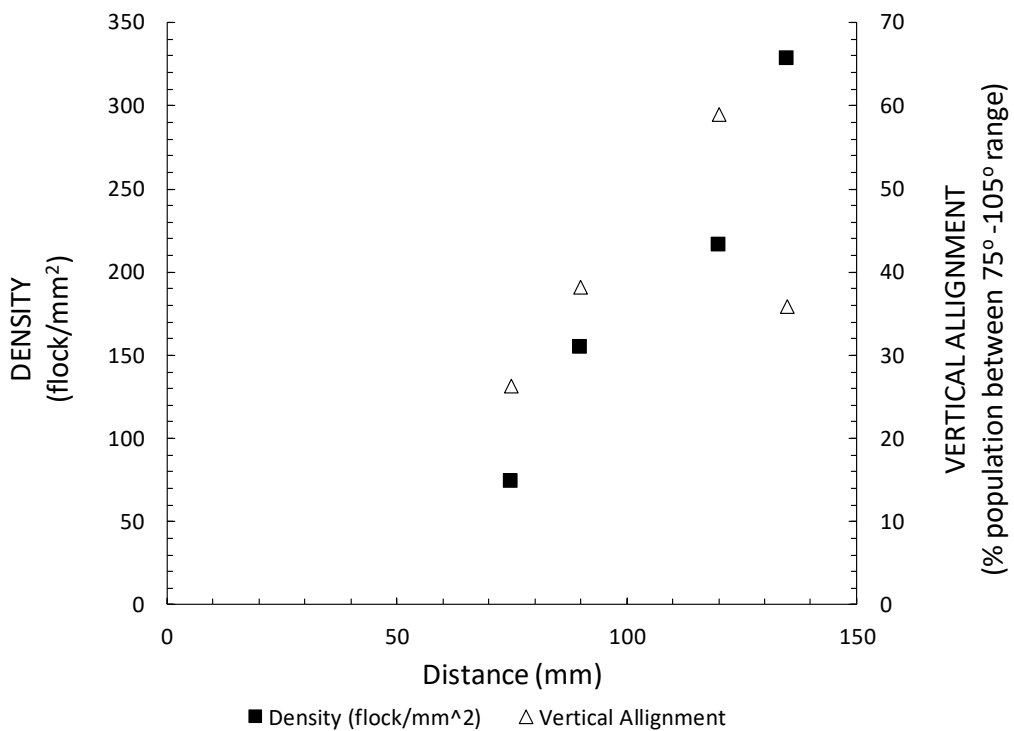


Figure 23 VA and areal density changes with respect to flight distance and more specifically X (distance between grid to top plate) for 0.4 mm N66 flocks (time and voltage is constant in all experiments).

Although setting a numerical criterion for areal density is relatively easy, the VA is rather a vague concept to materialize. Referring to the relevant literature, it was decided that the set of flocking conditions that lead to a VA of at least 50% of the counted population of flocks above the set “quality level” would be worth putting into further tests [29]. This quality level was set to a range between 75° to 100° in this work, where 90° being the absolute vertical (i.e. the flocking conditions that lead to a VA of $90^{\circ} \pm 15^{\circ}$ for at least 50% of the flocks would be used in producing mechanical test specimens).

In this group of experiments; up to 49% of the 0.6 mm flocks could be positioned between 75° to 100°, whereas up to 63% of the 0.4 mm flocks met the same criteria. As noted earlier several times, change in voltage, distance and field application time changes the flock density and VA. Besides these parameters, VA is also dependent on the physical properties of the flocks. It is known that as the length of the flocks increases, their vertical placement becomes easier due to the polarization of the charged flocks [29].

In interlaminar toughening studies, there had been a definite tendency towards using shorter flocks. As the feature sizes of the flocks approach the sizes of hills and troughs forming among the carbon fiber twills, both the epoxy impregnation levels can be expected to increase and mechanical properties in in-plane direction can be expected to remain unaffected. In addition, the thickness of the composite can possibly be controlled with better precision. Therefore, mechanical test specimens were prepared using 0.4 mm flocks. Representative SEM micrographs of 0.4 mm flocks with different areal densities and VA are given in Figure 24.

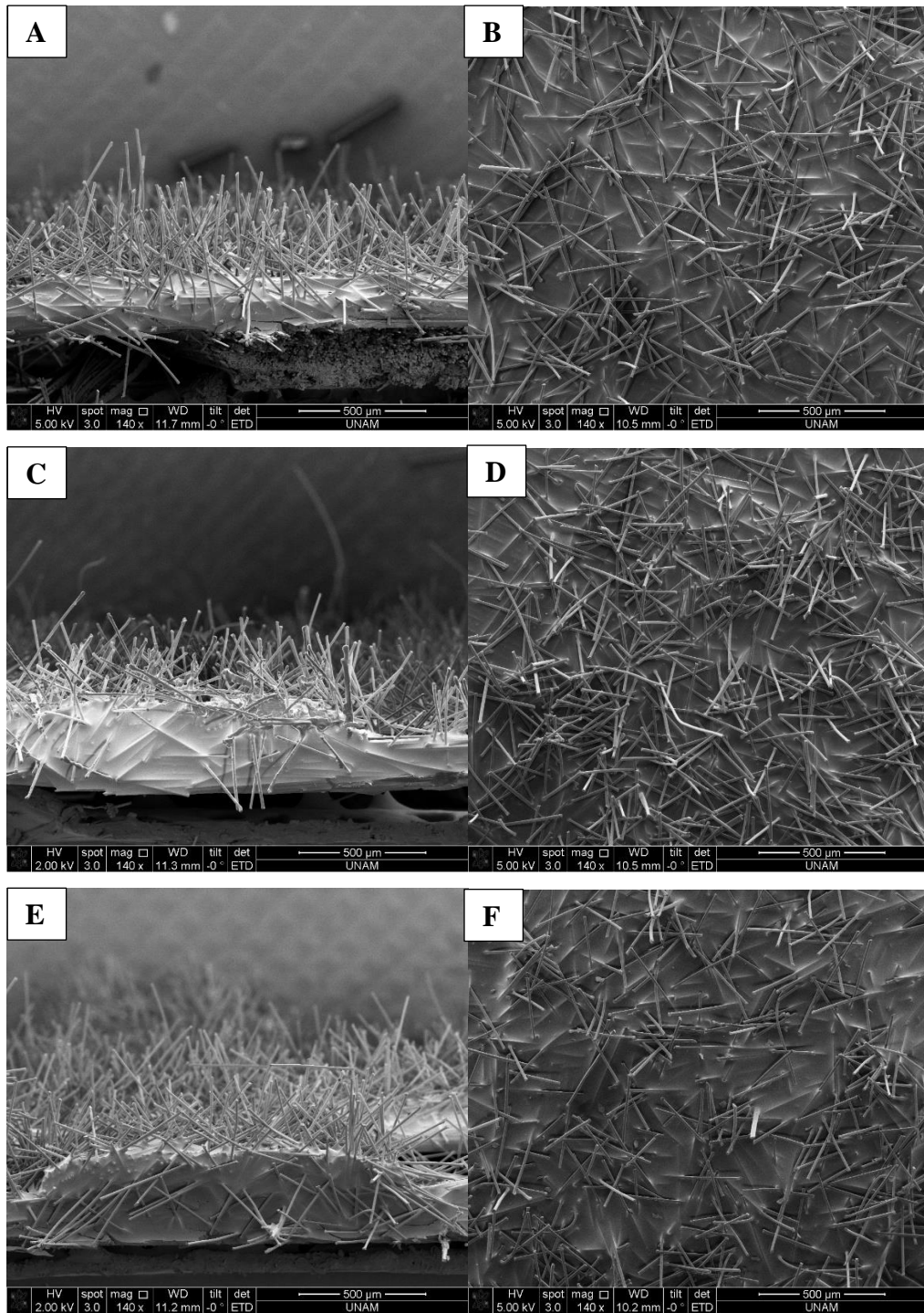


Figure 24 SEM images of 0.4 mm N66 flocks on prepreg surface; A-B (93 flocks/mm² – 63% VA), C-D (155 flocks/mm² – 38% VA), E-F (87 flocks/mm² – 44% VA)

4.2. Mode I Fracture Toughness Tests of Laminates

All samples used were prepared with similar flock densities on the surface (95 flocks/mm²). On the other hand, VA of flocks were varied and these composites were named as VA1 (33%), VA2 (48%), VA3 (64%). Composites interleaved with pristine 0.4 mm N66 flocks (R42-N66) and their silane-treated versions (R42-N66-S) were tested for their Mode I fracture toughness (G_{IC}) and improvements were compared against the non-intervened reference laminates.

4.2.1 Reference Laminates

During the studies, two different materials and ways were used to create initial cracks as described in Section 3.4. As a result of these changes, three reference composites were produced, two of which were produced using Teflon tape (R42 – B1 and B2) and the other with continuous polyester film (R42 – CF). Load – displacement curves obtained are given in Figures 25 – 27.

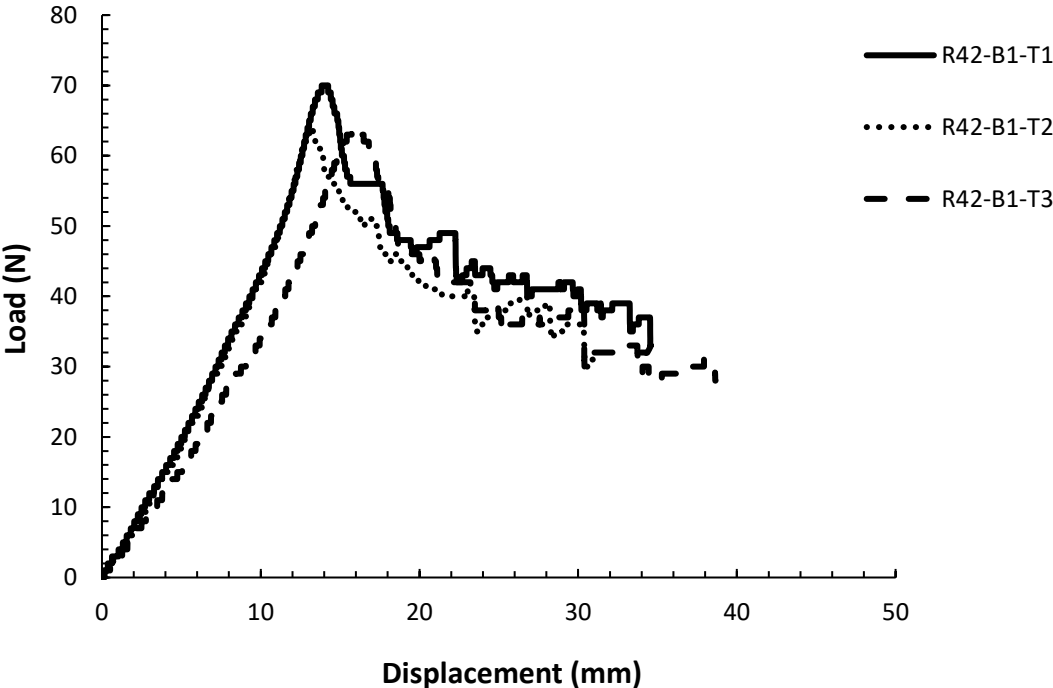


Figure 25 Load – displacement curve of the 1st reference plate using Teflon band (R42-B1).

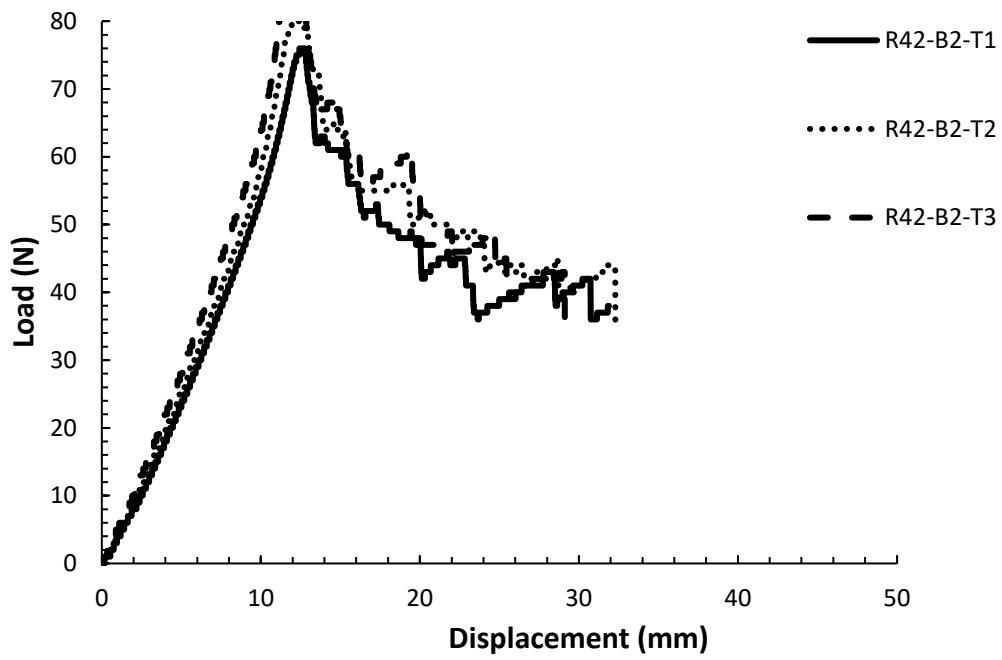


Figure 26. Load displacement curve of the 2nd reference plate using tefflon band(R42-B2).

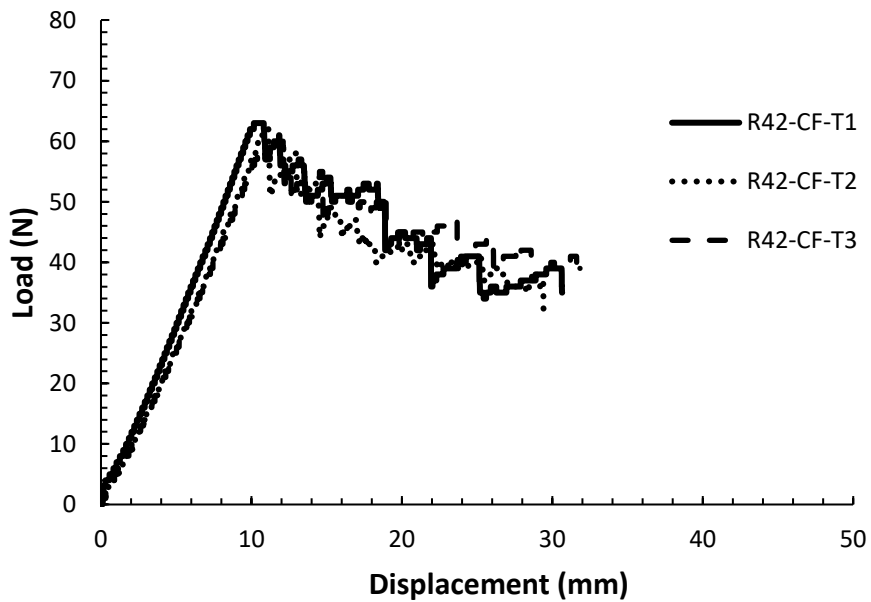


Figure 27 Load displacement curve of the reference plate using continuous film (R42-CF).

The initiation and propagation G_{IC} values of the reference plates were averaged from data presented in Figure 28. Teflon laid coupons were named as R42-B after further taking the average of R42-B1 and R42-B2. The averaged values were used for comparisons at later stages. The initiation G_{IC} values of the R42-B and R42-CF were 913 N/m and 665 N/m, respectively, whereas the propagation G_{IC} values of the same were 783 N/m and 628 N/m, respectively. It is important to note that use of a continuous film for crack initiation significantly improved the coupon to coupon reproducibility of the results. (Standard deviations of R42-B and R42-CF are 45 and 27 for $G_{IC}(init)$, 72 and 44 for $G_{IC}(prop)$)

Delaminated interfaces of the reference laminates revealed that the carbon fibers in the prepreg structures were separated directly from the epoxy similar to what had been reported for similar interfaces (Figure 29). Although small residue tips are indicative of a small amount of plastic strain, due to their limited extent the interfaces can be considered to be failing a brittle manner.

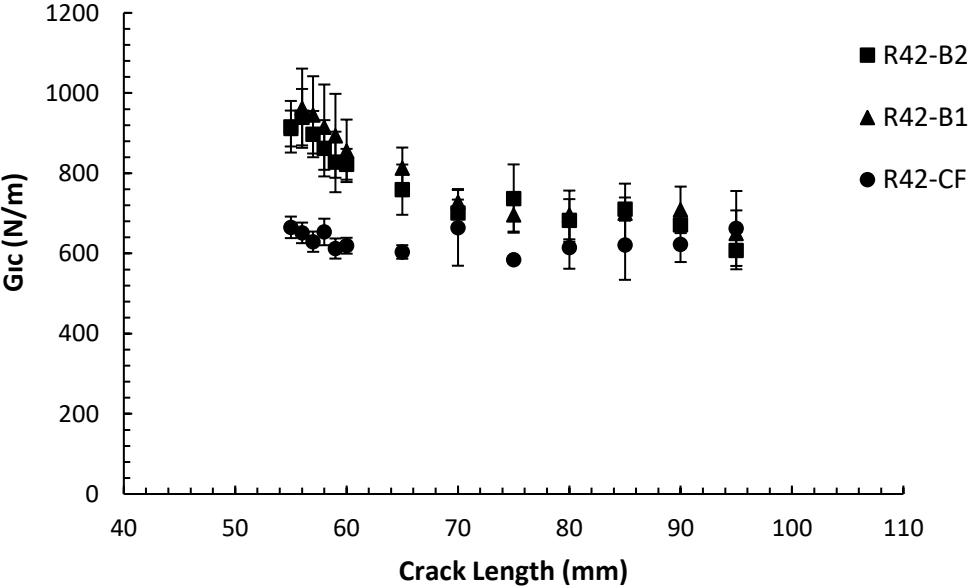


Figure 28 Variations of G_{IC} values of reference plates with crack length.

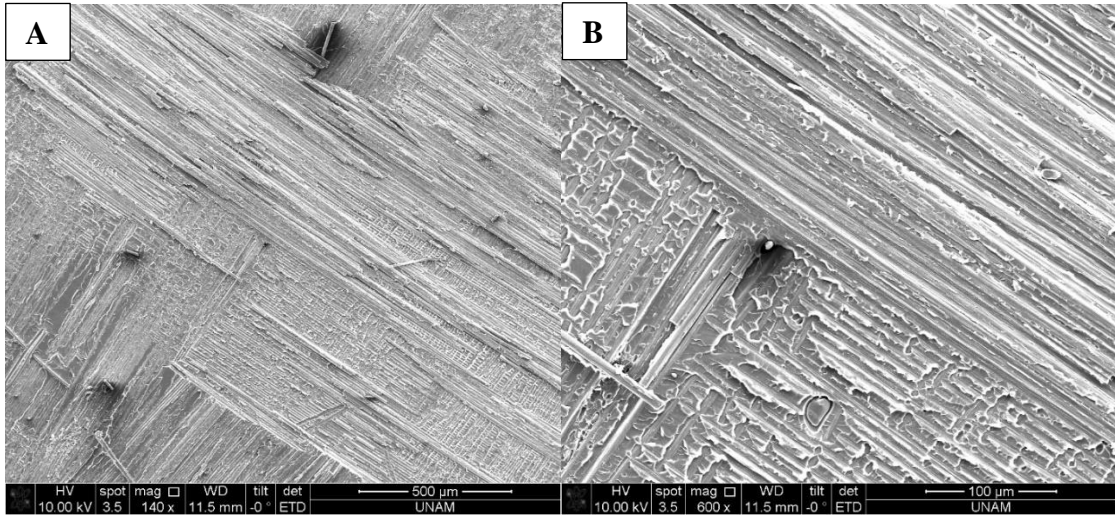


Figure 29 SEM image of fracture interfaces of reference plates (R42-B1), A ($\times 140$), B ($\times 600$)

4.2.2 0.4 mm N66 Flocked Composites (R42-N66)

Load – displacement curves of the composites flocked with untreated 0.4 mm N66 flocks are given in Figures 31-33.

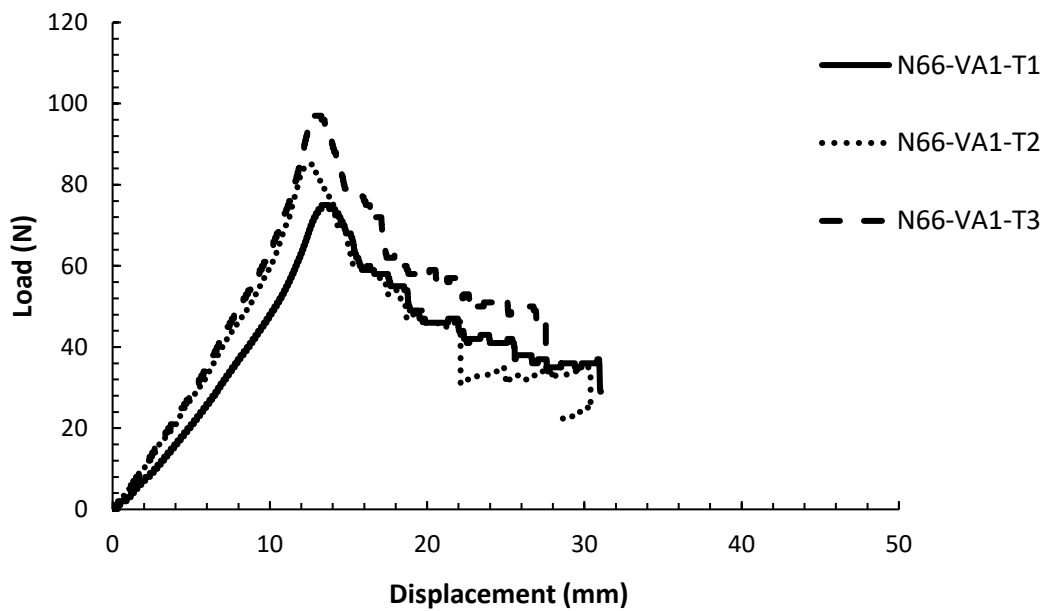


Figure 30 Load displacement curve of N66-VA1

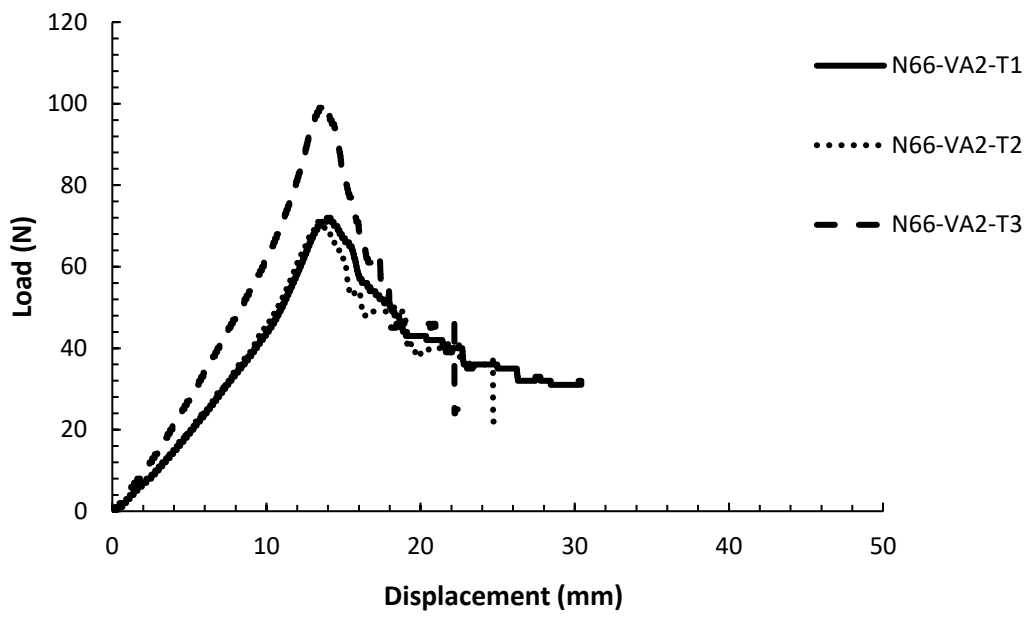


Figure 31 Load displacement curve of N66-VA2

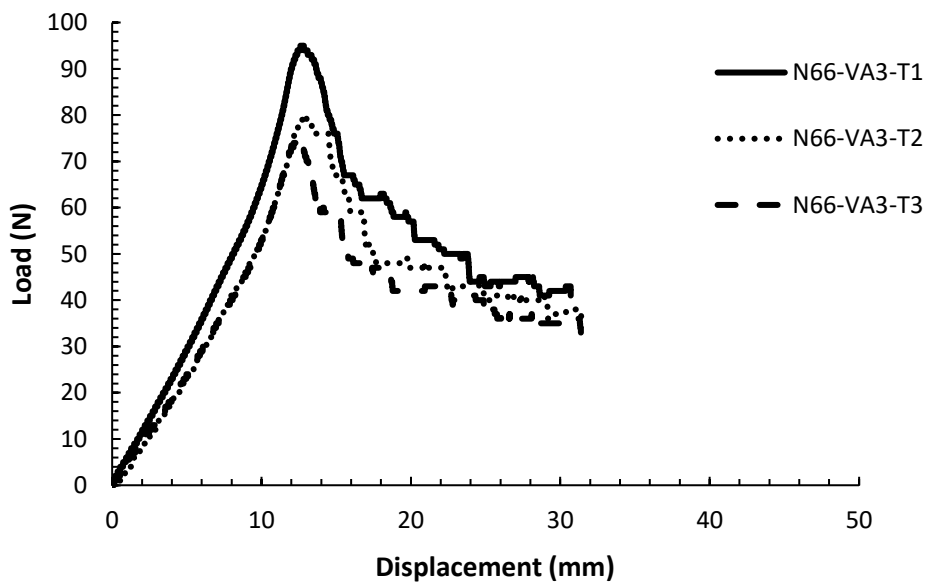


Figure 32 Load displacement curve of N66-VA3

The initiation and propagation G_{IC} values of the N66 flocked with three different VA levels were averaged from data and they are given in Table 4. As it can be seen from the Table 4, the increase in the VA of N66 flocks did not have a significant effect on neither the initiation nor the propagation values of G_{IC} , as opposed to what was expected. On the other hand, although areal densities were considered equal, VA2 was less dense than the others. The dips in both the initiation and propagation values of VA2 coincided better with the fact that, flock density might have had a stronger influence on the interfacial toughness, compared to that of VA. This may have its roots in the activated toughness mechanisms in these samples or the manufacturing defects caused by the slipping of the teflon tapes used while creating the pre-crack.

Table 4 G_{IC} values of 0.4mm N66 flock used laminates(N66).

	Flock density on surface (flock/mm ²)	Vertical Alignment (%)	G_{IC} initiation (N/m)	G_{IC} initiation (St.Dev.)	G_{IC} initiation (% change)	ΔG_{IC}^a (N/m)
R42-B	-	-	913	45	-	130
N66-VA1	112	33	1014	158	11	195
N66-VA2	88	48	981	129	7	271
N66-VA3	106	64	1020	137	12	195
	Flock density on surface (flock/mm ²)	Vertical Alignment (%)	G_{IC} propagation (N/m)	G_{IC} propagation (St.Dev.)	G_{IC} propagation (% change)	
R42-B	-	-	783	72		
N66-VA1	112	33	819	137	5	
N66-VA2	88	48	710	109	-9	
N66-VA3	106	64	825	92	5.4	

^a $\Delta G_{IC} = G_{IC}$ initiation- G_{IC} propagation

After Mode I fracture test, fracture interfaces cut with guillotine were examined with SEM (Figure 34). It was possible to see the debonding groves left from the smoothly peeled-off flocks, indicating little or no resistance against delamination through the chemical interaction of epoxy and N66 on the flock surfaces. Only improvement in these cases can be expected from the so-called “Velcro” effect, which is just based on the physical entanglement of the flocks; the better the VA, less the entanglement would be and the denser the flocks on the surface, more the entanglement would be. At higher densities also less slippage can be expected during the curing due to increased friction in shear mode.

An additional observation also clarified a worrisome point. The fact that flocking was applied only to one of the surfaces always brought about the doubt that, whether the epoxy would penetrate in between the flock during the curing or not. Observation of flocks sticking both to the bottom (flocked) and the top surfaces relieved that concern.

Relatively lower slopes observed in the elastic regions of the load – displacement curves call for a decreased stiffness of the interlaminar region. On its own, a lower stiffness cannot provide a better toughness. A higher stiffness accompanied with an intricate path for crack propagation generally leads to improved toughness values.

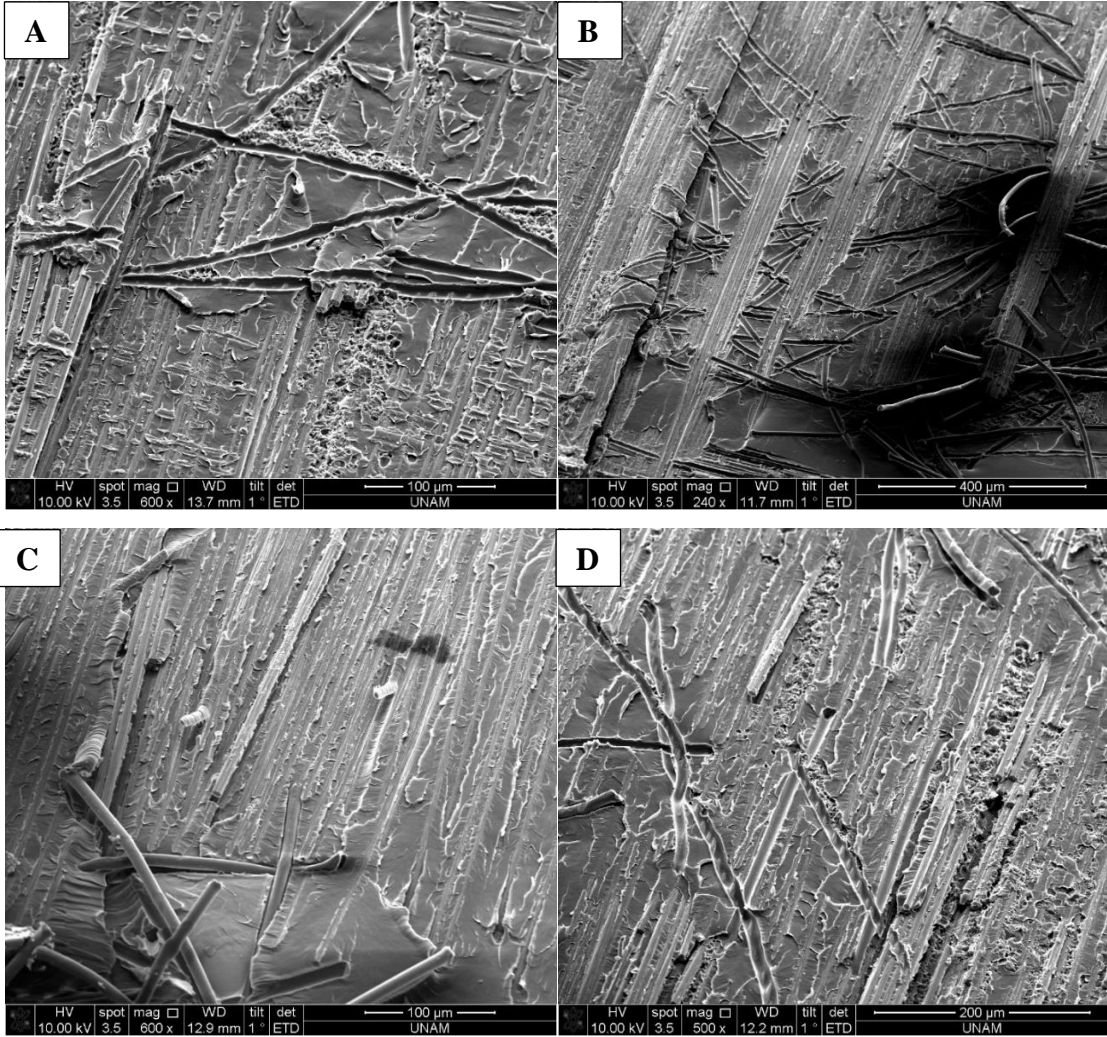


Figure 33 SEM images of fracture interface of 0.4 mm N66 flocked prepreg, A and B from bottom surface (flocked), C and D from top surface.

4.2.2 Silane Treated N66 Flocked Composites (R42-N66-S)

In order to increase the interaction of interlayer epoxy with flock surfaces, silane treatment of the flock was considered. Load – displacement curves of the composites flocked with silane treated N66 flocks (N66-S), are given in Figures 35-37 and results are summarized in Table 5.

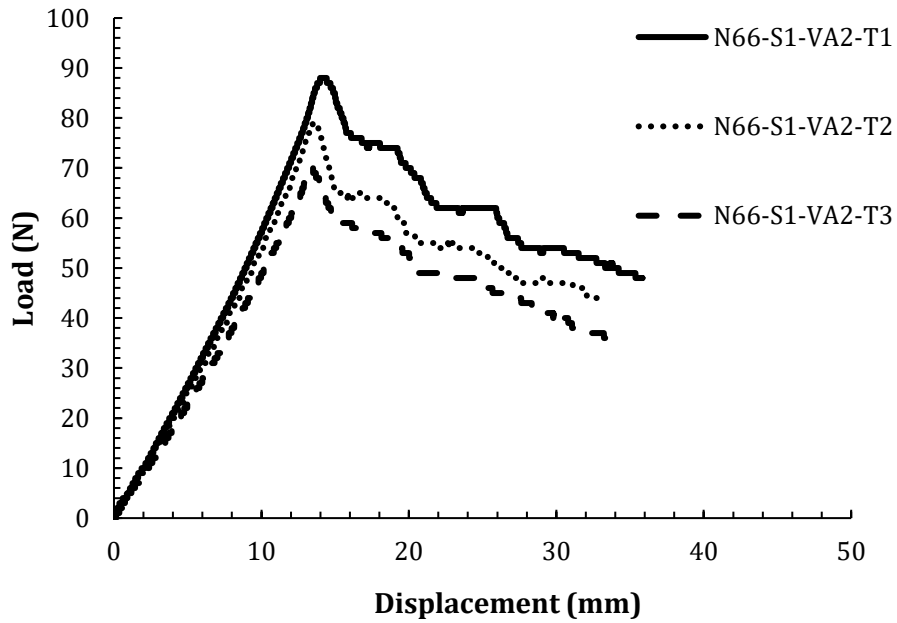


Figure 34 Load displacement curve of N66-S1-VA2.

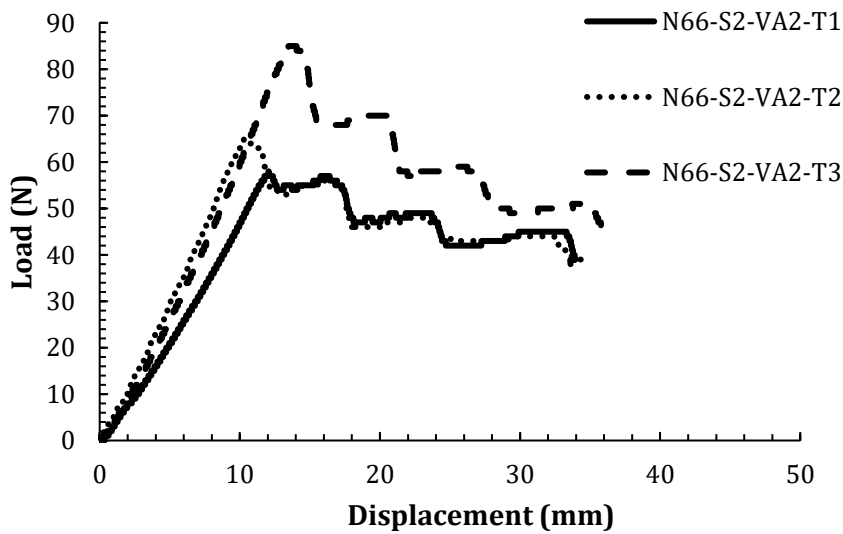


Figure 35 Load displacement curve of N66-S2-VA2

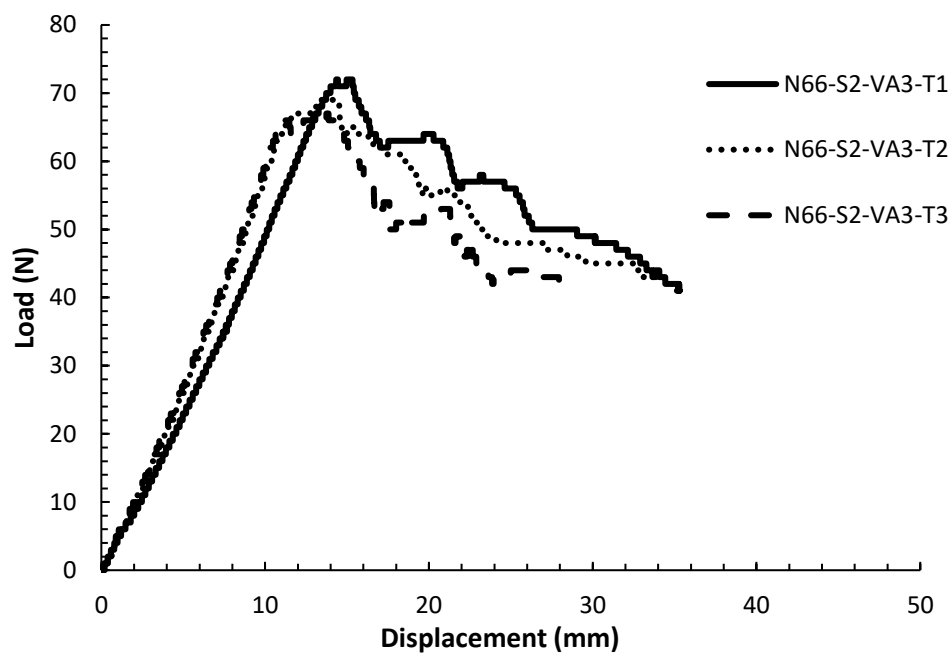


Figure 36 Load displacement curve of N66-S2-VA3

Table 5 GIC values of silane treated 0.4mm N66 flock used laminates(N66-S).

	Flock density on surface (flock/mm ²)	Vertical Alignment (%)	G _{IC} initiation (N/m)	G _{IC} initiation (St.Dev.)	G _{IC} initiation (% change)	ΔG _{IC} ^a (N/m)
R42-CF	-	-	665	27	-	37
N66-S2-VA2	88	48	781	240	17	-29
N66-S2-VA3	106	47	784	115	18	-65.18

	Flock density on surface (flock/mm ²)	Vertical Alignment (%)	G _{IC} propagation (N/m)	G _{IC} propagation (St.Dev.)	G _{IC} propagation (% change)
R42-CF	-	-	628	44	
N66-S2-VA2	88	48	810	227	29
N66-S2-VA3	106	47	849	101	35

^aΔG_{IC}= G_{IC} initiation- G_{IC} propagation

Silane treatment was applied on two different batches of N66 flocks. During the production of composites based on the first batch (N66-S1), Teflon which had been inserted during lay-up slipped. Although the values calculated were just estimations, the initiation and propagation GIC values of N66-S1 produced this way was 1053 N/m and 935 N/m, respectively. N66-S1 was produced with Teflon and it improved initiation and

propagation value of G_{IC} 13% and 16% with respect to N66-B. When the data of N66-S1 could have been corrected, improvements could potentially increase to 59% and 50%.

These observations were taken as positive signs of a promising surface modification. Therefore, a second batch of surface modified flocks was produced (N66-S2). For a better surface coverage on the bottom plate, the production was scaled up about two times and more flock was tried to be modified in one batch. In addition, to prevent the problems caused by the slipping of Teflon bands, the continuous film was used to create the precrack in experiments using the second batch of silane treated N66 flocks. Therefore, N66-S2-VA2 and VA3 were compared against R42-CF. The initiation and propagation G_{IC} values were averaged from data and summarized in Table 5.

Results of G_{IC} indicated that silane might not have been homogeneously interacted with the N66 flocks on surface. The improvements remained modest. However, the resistance against crack propagation was much higher in the propagation. This can especially be important in fatigue based designs. Nevertheless, if the limitations on batch sizes could be overcome and the flocking could be performed with enough flocks in the bottom plate, the whole potential of silane treatment could be gaged.

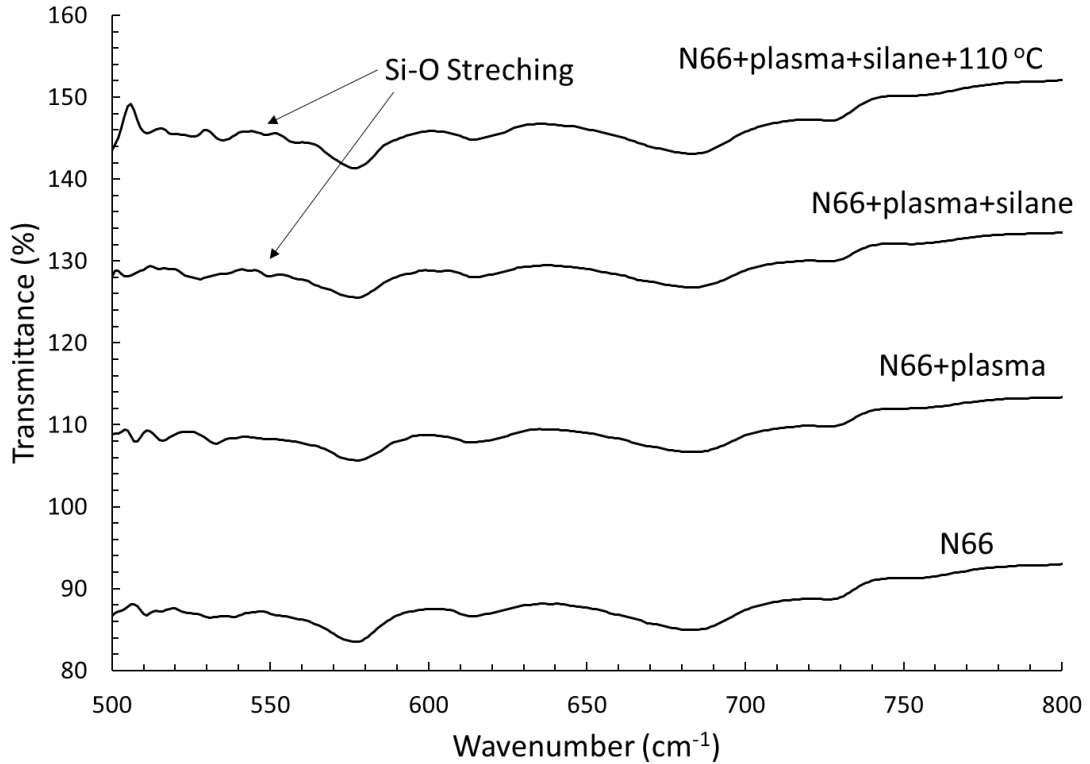


Figure 37 FTIR results of N66 flocks and all steps of silanization.

In Figure 38, in order from bottom to top, FTIR spectra of N66, oxygen plasma treated N66, silane treated N66 and N66 kept at 110°C after silane treatment are given. When the amount of silane that might be residing on N66 is considered, it can be expected that there would be no intense Si-O stretching absorptions. As shown in the figure, a small trace of Si-O band can be observed after the treatment. This shows that a certain amount of silane adheres to the surface.

On the surface of the flocks, adhered and broken epoxy residues were visible in Figures 39 – A, B, C in. It can be observed from the flocks designated by the red circles (in Figures 39 – A, C, D, E) that the bridging mechanism can triggered. This can be evidenced by the broken flock tips that had possibly been a position holding on the upper and lower layers from both ends of the flock. It was also observed that while the crack propagates, flocks were positioned vertically and they broke along their stronger axes. In Figure 39 – A, there are some traces on flocks that were indicated by the blue circle. These traces show that silane increases the adhesion of N66 flocks to epoxy. Also, this flock was likely to be peeled-off from surface gradually. There were a number of similarly detached flocks with plenty of epoxy fragments left adhered to the flocks after failure. These observations strongly suggest that the silane treatment increased the debonding resistance of the flocks.

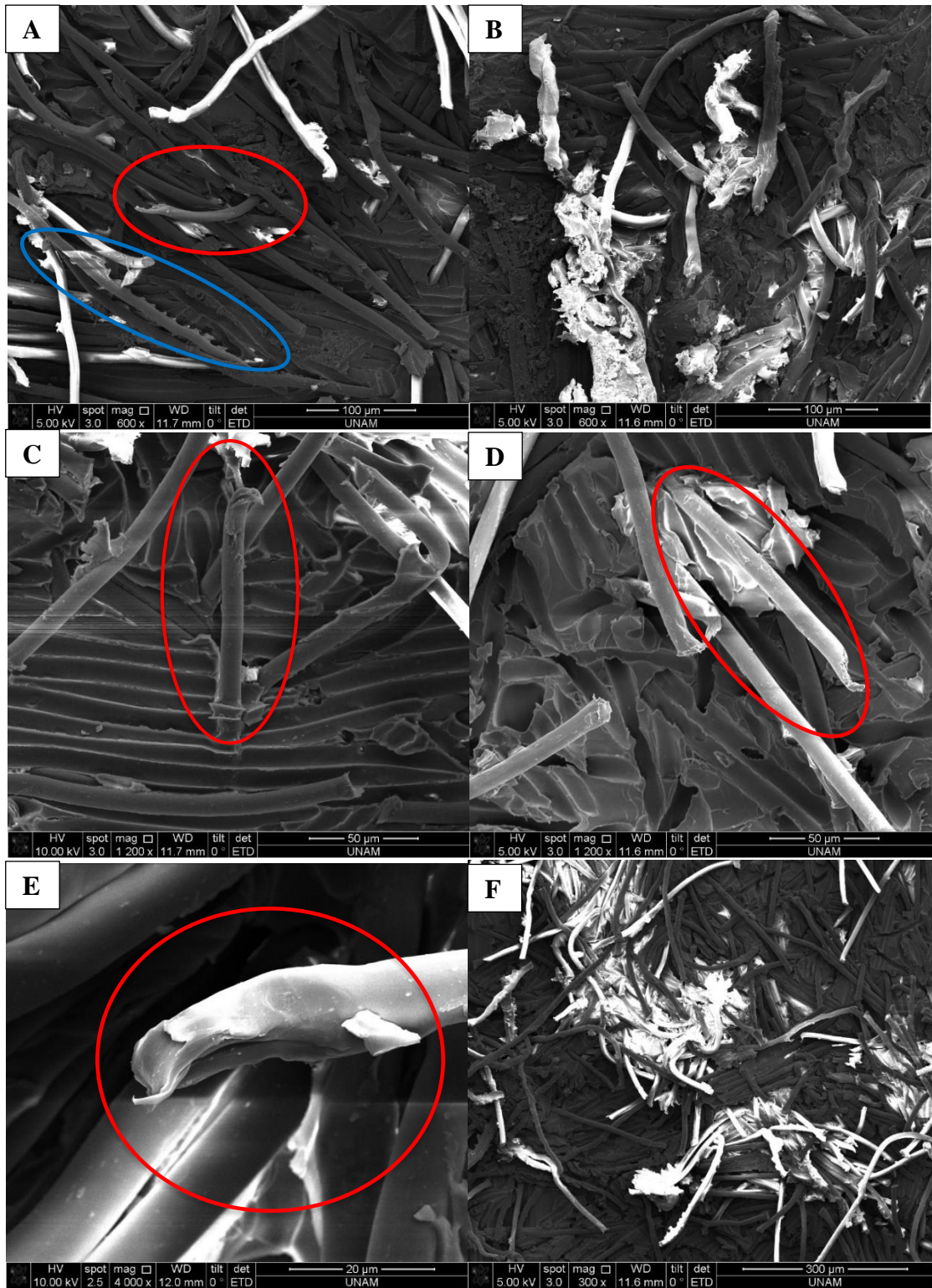


Figure 38 SEM images of silane treated N66 flocked laminate's fracture surface.

5.CONCLUSIONS

1. Flocking of 0.4 mm long, 0.9 dtex, only dispersant coated N66 flocks onto carbon fiber prepregs can be achieved through compulsory modifications to the flocking cabin and fine-tuning of the electrical field applied to the flocks at different levels of field application time, voltage and both bottom and target plate separation distance ($X+Y$) and the ratio of the distances of the mid-grid to these plates (Y/X).
2. Conditions favoring higher areal densities and higher vertical alignment (VA) were explored.
3. A numerical quality measure for the vaguely defined VA was developed. Flocking conditions leading to at least 50% of the flocks to reach a VA of $90^{\circ}\pm 15^{\circ}$ was considered favorable for the proceeding study on interlaminar toughening.
4. Both the density and VA were maximized by increasing the applied voltage (65 kV), time (7 sec.) and adjusting distance between plates ($Y/X=1$, $X+Y=180\text{mm}$).
5. G_{IC} values of composites could be increased up by 13% and 16% in crack initiation and propagation stages, respectively with the use of 0.4 mm long, 0.9 dtex N66 flocks.
6. The failure analyses results indicated that the delamination was hindered only via debonding at the flock – epoxy interface. Smooth peel grooves showed that the chemical interaction of the flock and the matrix remained limited. Therefore, improvements were presumed to be rather the result of physical entanglements of the flocks and they correlated better with the areal densities of the flocks rather than their VA.
7. Increasing the interaction of epoxy with N66 flocks was possible with the amine group functionalities that could be imparted on the flock surfaces via APTES, that were presumed to be covalently interacted with the hydroxyl functionalized N66 surfaces treated under oxygen plasma.
8. There had been some limitations faced on either the crack initiation tab placement or the scale-up of the silanization process of the flocks and

therefore a perfectly executed set of mechanical test results with aminosilane functionalized flocks could not be collected. Nevertheless, by using aminosilane treated 4 mm 0.9 dtex N66 flocks, initiation and propagation G_{IC} values of layered composites were improved by 18% and 35%, respectively. Improvements being about twice in the propagation stage is a promising attribute for designing against fatigue.

9. The delaminated interfaces proved the strong interaction between the epoxy and fibers, which hindered the easy peel-off of the flock from the matrix. With better specimen preparation practices and a refined scale-up process for silanization step, better results can be achieved in Mode I fracture toughness values.

6. REFERENCES

1. Zimmermann, N. and P.H. Wang, A review of failure modes and fracture analysis of aircraft composite materials. *Engineering failure analysis*, 2020. 115: p. 104692.
2. Mangalgi, P., Composite materials for aerospace applications. *Bulletin of Materials Science*, 1999. 22(3): p. 657-664.
3. Gopal, K., Product design for advanced composite materials in aerospace engineering, in *Advanced composite materials for aerospace engineering*. 2016, Elsevier. p. 413-428.
4. Siddique, A., et al., Mode I fracture toughness of fiber-reinforced polymer composites: A review. *Journal of Industrial Textiles*, 2019: p. 1528083719858767.
5. Zeng, Y., et al., Improving interlaminar fracture toughness of carbon fibre/epoxy laminates by incorporation of nano-particles. *Composites Part B: Engineering*, 2012. 43(1): p. 90-94.
6. Wu, X.F. and A.L. Yarin, Recent progress in interfacial toughening and damage self - healing of polymer composites based on electrospun and solution - blown nanofibers: An overview. *Journal of applied polymer science*, 2013. 130(4): p. 2225-2237.
7. Ranatunga, V. and S.B. Clay, Interlaminar Fracture Toughness Characterization of Z-Pinned and Flocked Composite Laminates, in *55th AIAA/ASME/ASCE/AHS/ASC Structures, Structural Dynamics, and Materials Conference*. 2014.
8. Kılıcoglu, M., Use of Nano-Hybrid Systems in Carbon Fiber Reinforced Polymer Matrix Composites(CFRP) for Interfacial Toughening. 2018.
9. Fodor, K.F., et al., Dynamic mechanical behavior of flocked layer composite materials. *Composite Structures*, 2019. 207: p. 677-683.
10. Khan, R., Fiber bridging in composite laminates: A literature review. *Composite Structures*, 2019: p. 111418.
11. <Pinto_et_al-2014-Polymer_Composites.pdf>.

12. Daelemans, L., et al., Damage-resistant composites using electrospun nanofibers: a multiscale analysis of the toughening mechanisms. *ACS applied materials & interfaces*, 2016. 8(18): p. 11806-11818.
13. Pegorin, F., K. Pingkarawat, and A. Mouritz, Comparative study of the mode I and mode II delamination fatigue properties of z-pinned aircraft composites. *Materials & Design (1980-2015)*, 2015. 65: p. 139-146.
14. Kim, Y.K. and A. Lewis, Through-Thickness Reinforcement of Laminar Composites. *Journal of Advanced Materials -Covina*, 2017.
15. Liu, L., et al., Optimal design of superfine polyamide fabric by electrostatic flocking technology. *Textile Research Journal*, 2011. 81(1): p. 3-9.
16. Campbell, F.C., *Structural composite materials*. 2010: ASM international.
17. Cherian, A.B., L.A. Varghese, and E.T. Thachil, Epoxy-modified, unsaturated polyester hybrid networks. *European Polymer Journal*, 2007. 43(4): p. 1460-1469.
18. Wu, X., *Fracture of Advanced Polymer Composites with Nanofiber Reinforced Interfaces (PhD Thesis)*. University of Nebraska-Lincoln, Lincoln, Nebraska, USA, 2003.
19. AC09036782, A., Standard test method for mode I interlaminar fracture toughness of unidirectional fiber-reinforced polymer matrix composites. 2007: ASTM Internat.
20. Wang, W.-T., et al., Effect of the characteristics of nylon microparticles on Mode-I interlaminar fracture toughness of carbon-fibre/epoxy composites. *Composites Part A: Applied Science and Manufacturing*, 2020. 138: p. 106073.
21. Huang, Y., et al., Interlaminar fracture toughness of carbon-fiber-reinforced epoxy composites toughened by poly (phenylene oxide) particles. *ACS Applied Polymer Materials*, 2020. 2(8): p. 3114-3121.
22. Sager, R.J., A characterization of the interfacial and interlaminar properties of carbon nanotube modified carbon fiber/epoxy composites. 2010, Texas A & M University.
23. Pinto, M., et al., Improving the strength and service life of jute/epoxy laminar composites for structural applications. *Composite Structures*, 2016. 156: p. 333-337.
24. Kim, M., et al., Property enhancement of a carbon fiber/epoxy composite by using carbon nanotubes. *Composites Part B: Engineering*, 2011. 42(5): p. 1257-1261.

25. Saghafi, H., et al., The effect of interleaved composite nanofibrous mats on delamination behavior of polymeric composite materials. *Composite Structures*, 2014. 109: p. 41-47.
26. Jia, R., Y.K. Kim, and J. Rice, Comparing the fracture toughness of 3-D braided preform composites with z-fiber-reinforced laminar composites. *Textile Research Journal*, 2010. 81(4): p. 335-343.
27. Bolgen, S.W., Flocking technology. *Journal of Coated Fabrics*, 1991. 21(2): p. 123-131.
28. Kim, Y.K., Flocked fabrics and structures, in *Specialist Yarn and Fabric Structures*. 2011. p. 287-317.
29. Yu, Z., S. Wei, and J. Guo, Fabrication of aligned carbon-fiber/polymer TIMs using electrostatic flocking method. *Journal of Materials Science: Materials in Electronics*, 2019.
30. Uetani, K., et al., Elastomeric thermal interface materials with high through-plane thermal conductivity from carbon fiber fillers vertically aligned by electrostatic flocking. *Adv Mater*, 2014. 26(33): p. 5857-62.
31. Sun, Y., et al., Improvement of out-of-plane thermal conductivity of composite laminate by electrostatic flocking. *Materials & Design*, 2018. 144: p. 263-270.
32. Ren, X., et al., A Self - cleaning Mucus - like and Hierarchical Ciliary Bionic Surface for Marine Antifouling. *Advanced Engineering Materials*.
33. Li, X., et al., Three-dimensional stretchable fabric-based electrode for supercapacitors prepared by electrostatic flocking. *Chemical Engineering Journal*, 2020: p. 124442.
34. Ji, T., et al., Thermal conductive and flexible silastic composite based on a hierarchical framework of aligned carbon fibers-carbon nanotubes. *Carbon*, 2018. 131: p. 149-159.
35. Measurements of Reflectance and Thermal Emissivity of a Black Surface Created by Electrostatic Flocking with Carbon-Fiber Piles.
36. O'Donnell, J., et al., Electro-mechanical studies of multi-functional glass fiber/epoxy reinforced composites. *Journal of Reinforced Plastics and Composites*, 2019.

APPENDIX

APPENDIX 1 – Example of DCB test data processed according to ASTM-D5528

As explained in the thesis, during the interface toughening studies, Mode I Fracture toughness measurements were carried out in the direction of was applied accordingly.

At the end of this test, the initial and progressive fracture toughness of the composite material was determined by plotting the GIC characterizing it as a function of crack length, resistance curve is created.

At least 3 samples are tested for one test. Two samples of each sample before starting the test. its side is white from the point where the insert (teflon or continuous film) ends (Figure 40 red arrow) painted with correction fluid. Pre-crack point 5 mm after the end point of Teflon after the first 5 mm, every 1 mm marked, the next 45 mm must be marked every 5 mm.



Figure 39 Painted DCB coupon.

After the sample is prepared, the loading blocks are attached to the sample (Figure 41A) and inserted into the device (Figure 41B).

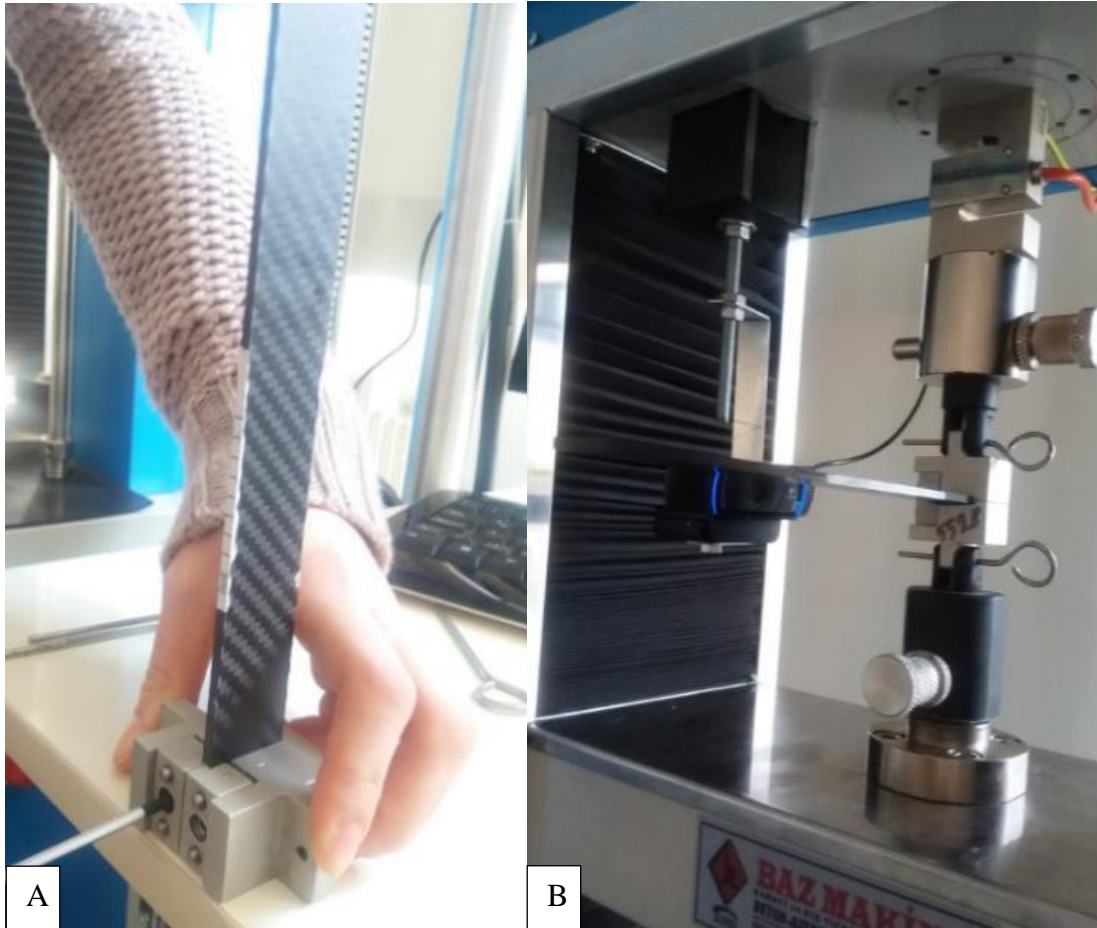


Figure 40 Sample inserting to mechanical testing device.

The value pair in “a teflon” is first recorded on the page where it will be saved and the test is started. While values are recorded in one of the windows, in the other load – elongation graph is formed. Crack in the sample each time it reaches the points marked on it, the load – elongation for the relevant crack size value pair must be saved. Images from the crack progression Figure 42-A and it is given in Figure 42- B.

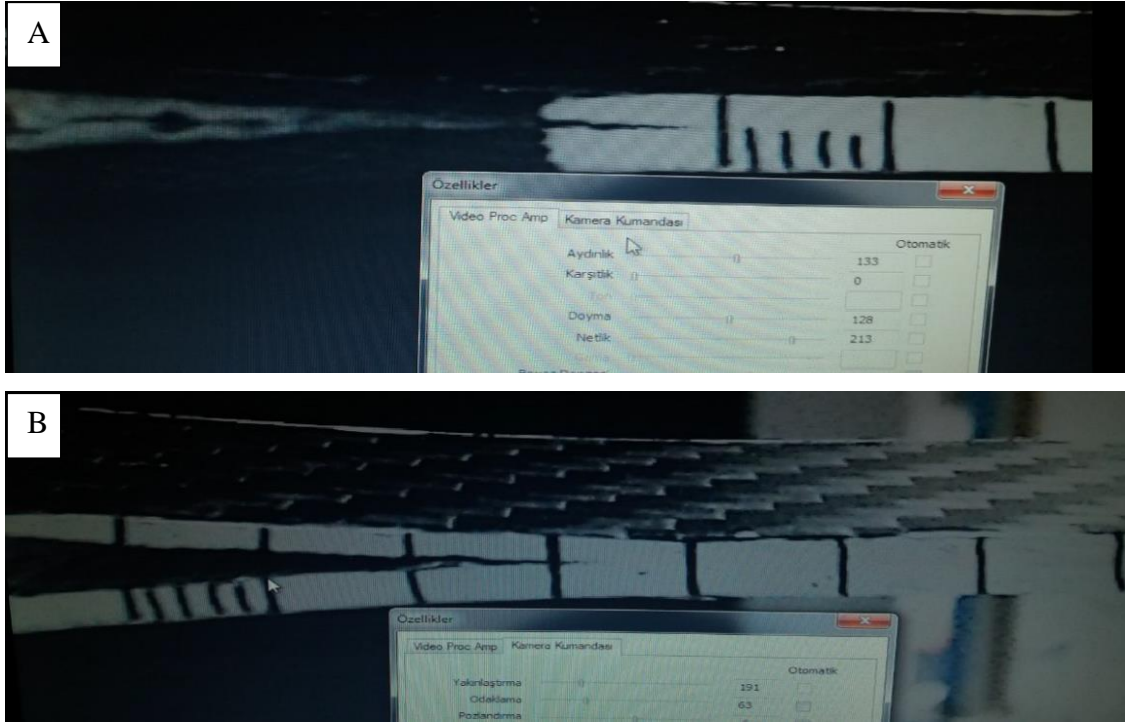


Figure 41 Crack propagation on sample.

At the end of the test, the load (P) and elongation (d) values in column at the table on the right of Figure 8, are transferred to Excel and calculations are made for each sample. Crack length (a), load (P) and extension (d) values are copied to the appropriate columns in Excel, after the test was completed for 3 sample (Figure 43),

	a [mm]	P [N]	d [mm]
1	a10n	49.7	53
2	a10e-crack	5	55
3	a10 VIS	5	56
4	a1	6	64
5	a2	7	60
6	a3	8	52
7	a4	9	53
8	a5	10	50
9	a6	15	44
10	a7	20	36
11	a8	25	29
12	a9	30	22
13	a10	35	21
14	a11	40	11
15	a12	5	19

Figure 42 Recorded, a,P,d values.

After a, P and d values are placed in the appropriate column (Figure 44 C, D, E column) in Excel, then the GIC value (M column) is calculated. However, intermediate calculations are required before calculating the GIC value. To calculate the GIC Modified Beam Theory is used. The equation applied in this theory is also in the text of the thesis.

	B	C	D	E	F	G	H	I	J	K	L	M	N
	a(mm)	P(N)	d(mm)	t(s)	G(J/m ²)	C			C ^(1/3)	a (m)	a (mm)	G(J/m ²)	
1	a teflon	47	76	11.0099528	658.58		0		0				
2	a pre-crack	5	72	13.8080316	696.8	639.51	0		0			890.043219	
3	a0 VIS	5	74	13.8175444	696.93	603.4	0.187		0.572	0.052	52	915.396854	
4	a1	6	74	13.852256	741.79	619.36	0.187		0.572	0.053	53	903.461082	
5	a2	7	75	14.4671472	742.36	336.13	0.193		0.578	0.054	54	941.708072	
6	a3	8	75	14.7360356	745.5	332.29	0.196		0.581	0.055	55	944.779167	
	a4	9	75	14.9010928	745.5	327.44	0.199		0.584	0.056	56	941.20091	
8	a5	10	75	15.3937344	746.57	322.69	0.205		0.590	0.057	57	958.116249	
9	a6	15	66	17.4300808	748.85	300.89	0.264		0.642	0.062	62	889.7025	
10	a7	20	65	21.1718496	947.89	421.67	0.326		0.688	0.067	67	996.502697	
11	a8	25	61	23.4448016	1035.63	324.34	0.384		0.727	0.072	72	973.541796	
12	a9	30	54	26.5001308	1113.91	328.47	0.491		0.789	0.077	77	919.079681	
13	a10	35	53	29.2616764	1286.33	358.54	0.552		0.820	0.082	82	942.777416	
14	a11	40	51	31.9328504	1455.65	368.64	0.626		0.856	0.087	87	939.743434	
15	a12	45	46	35.27832	1518.9	333.8	0.767		0.915	0.092	92	891.160198	
	a13												
17	a14												
18	a15												

Figure 43 Excell table of P,a,d values

To obtain the Δ value, the 'compliance' C value (column H) is used. It is equal to δ/P . The value of $C^{1/3}$ (J column) corresponds to the layer separation lengths (L column). In the graph against which it is drawn, the point where the graph cuts the x-axis gives the value Δ . "a" value in the column is marked on the initial crack size and the sample. is equal to the sum of the propagating instantaneous crack length The L column is in the K column. values are calculated in meters. The graph shown below was drawn using the values in the J and L column and the point that intersects the x-axis of the graph is replaced by y in the equation circled in red calculated by putting zero (Figure 45).

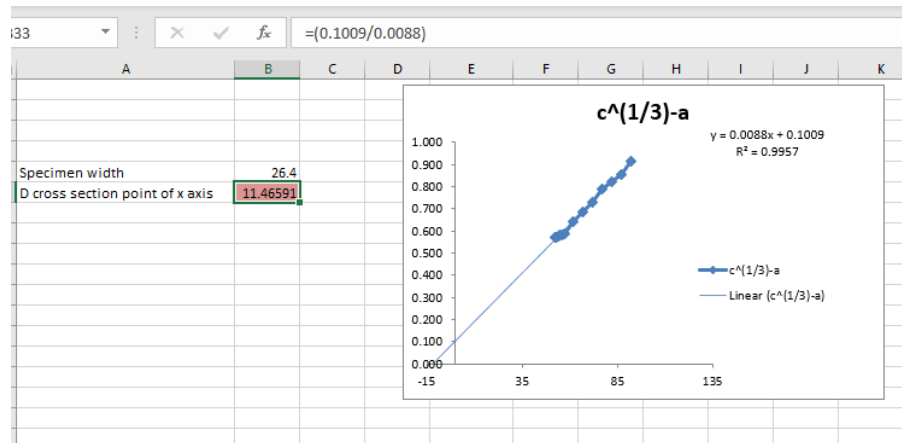


Figure 44 Calculation of Δ .

For each sample, a (mm) in column L and M shown in Figure 46 and G_{IC} (N/m) – a (mm) and the average of all sample’s values are taken, and their graphs are drawn with their standard deviations. All in the example The G_{IC} values of the samples together with the crack lengths are in Excel below shown. In addition, the average of the crack length and G_{IC} values at the end (Figure 46 G, I column) and standard deviation values (H and J column) calculated.

A	B	C	D	E	F	G	H	I	J	K
a1	T1	a2	T2	a3	T3	avg.	s.d.	avg.	s.d.	
52	915.3969	52	733.9637	53	702.984	784.11	114.7439	52.3	0.57735	
53	903.4611	53	724.0292	54	700.4704	775.99	111.0225	53.3	0.57735	
54	941.7081	54	780.5414	55	691.858	804.70	126.6652	54.3	0.57735	
55	944.7792	55	798.96	56	798.2554	847.33	84.39287	55.3	0.57735	
56	941.2009	56	902.133	57	807.1035	883.48	68.96742	56.3	0.57735	
57	958.1162	57	910.2971	58	830.2818	899.57	64.58942	57.3	0.57735	
62	889.7025	62	903.352	63	758.9631	850.67	79.71537	62.3	0.57735	
67	996.5027	67	904.0232	68	683.3451	861.29	160.8928	67.3	0.57735	
72	973.5418	72	900.5912	73	789.6745	887.94	92.58462	72.3	0.57735	
77	919.0797	77	852.4152	78	695.7592	822.42	114.6424	77.3	0.57735	
82	942.7774	82	875.3953	83	721.6622	846.61	113.3329	82.3	0.57735	
87	939.7434	87	897.3227	88	727.8515	854.97	112.1147	87.3	0.57735	
92	891.1602	92	913.5113	93	764.9101	856.53	80.12593	92.3	0.57735	
avg.	936.81	863.55	747.51	849.29	100.7538	G1C init: 784 N/m G1C prop: 849 N/m				
s.d.	31.19	69.64	50.15	50.33	50.33					

Figure 45 Calculation of average G_{IC} values from 3 samples

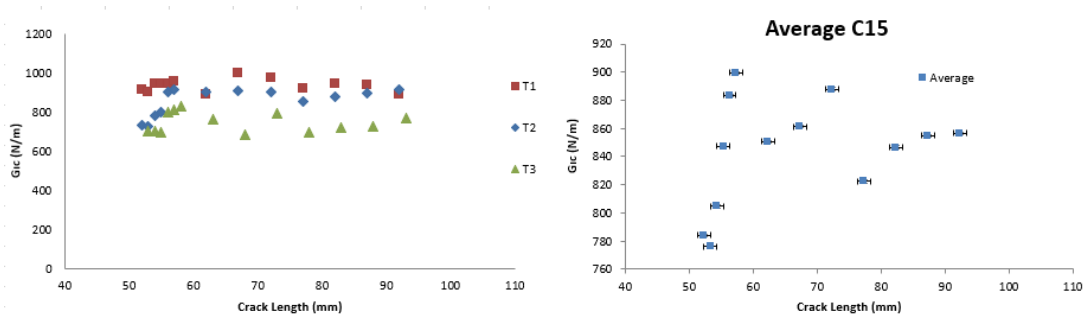


Figure 46 GIC – a” graphs with average and standard deviations.

APPENDIX 2 – Determination of flock density and vertical alignment on the prepreg

ImageJ program was used for quantifying densities and vertical alignments.

Measurement of Density

The dimensions of the top view SEM images were calibrated on a pixel basis with IMAGE J, to determine the $1 \times 1 \text{ mm}^2$ area exactly. $1 \times 1 \text{ mm}^2$ square area are cropped and flocks are count in that area (Figure 48). Number of flocks is recorded in units of flocks/ mm^2 .

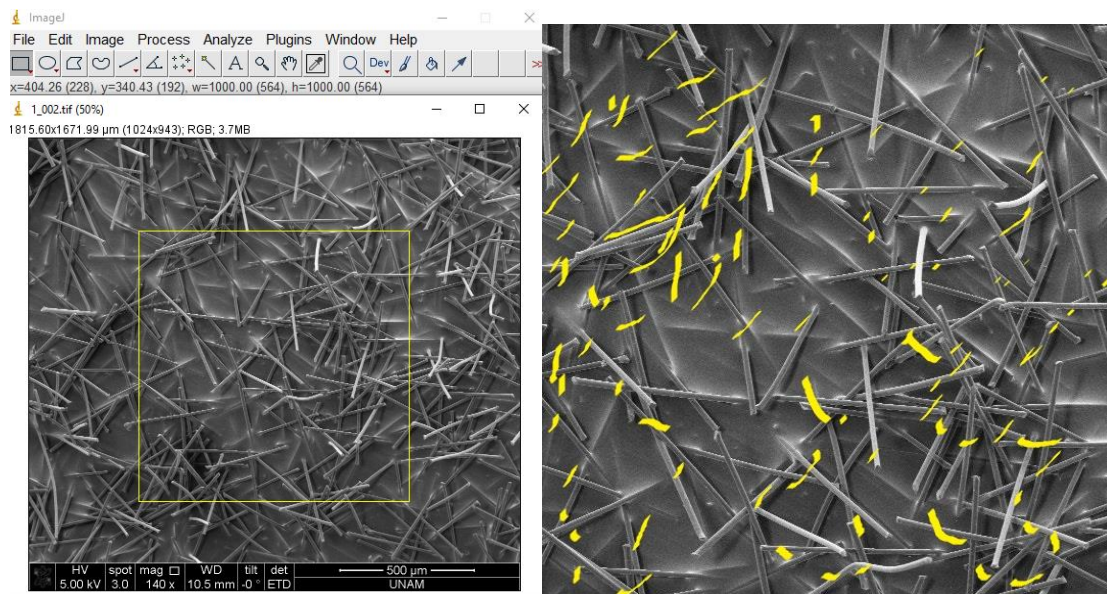


Figure 47 Top view of flocked surface.

Measurement of Vertical Alignment

Side view SEM images of 10×10 mm² cut prepregs, allows to measure angle between flocks and prepreg surface. While the cut prepreg taken from the surface, orientation of the flocks change. Therefore, the angles of the flocks below the line shown are not measured. (Figure 49)

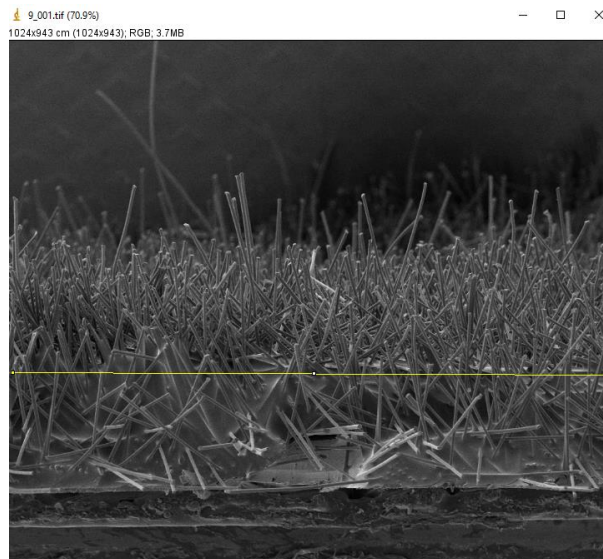


Figure 48 SEM image of flocked prepreg.

While the angles between the prepreg surface and the flocks are given, the positive angle with the horizontal plane is taken. The angles of 50 to 100 flocks were measured according to the number of flocks that can be clearly seen on the surface (Figure 50).

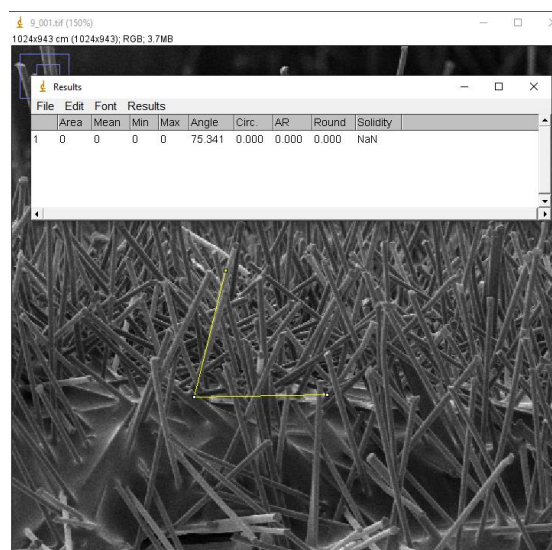


Figure 49 Angle measurement of flocks.

All measurements were exported to Excel to determine the percentage of upright flocks in the total population. With the

"=COUNTIF(B2:B68,">=75")-COUNTIF(B2:B68,">=105")" function on Excell, the number of flocks making an angle between 75 and 105 degrees with the surface was obtained. The number of these flocks was divided by the total number of flocks measured, and the percentage of upright flocks to the total population was determined.

(Figure 51)

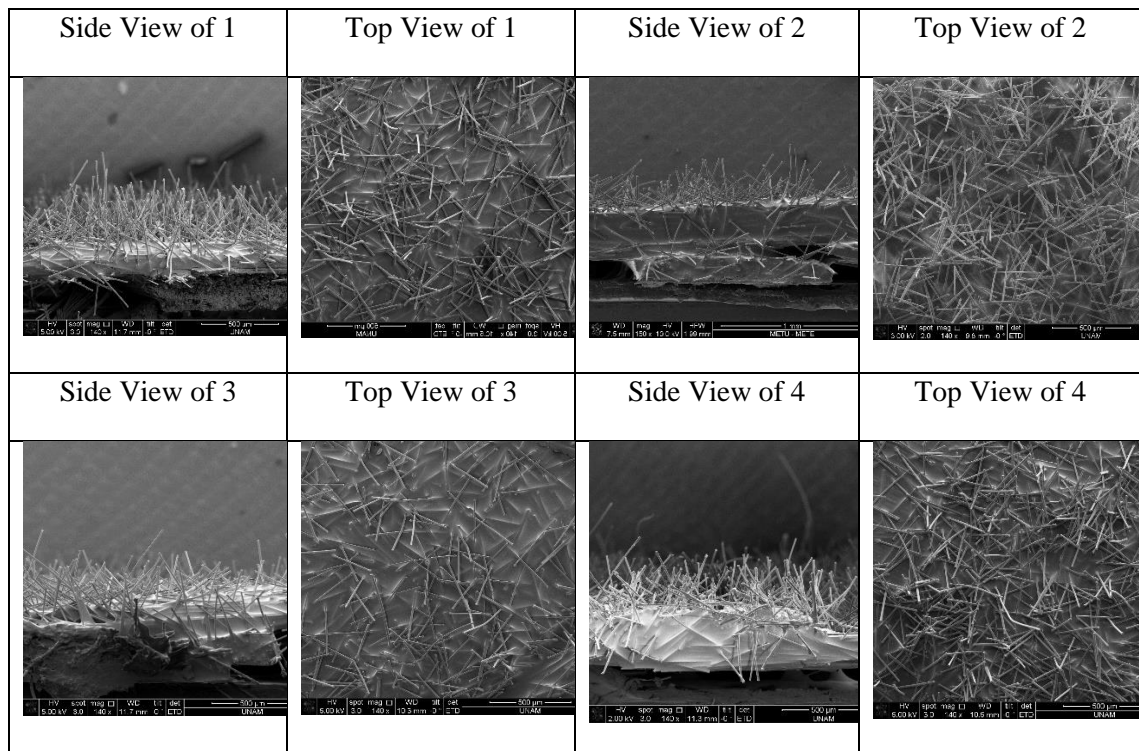
	A	B	C	D	E
1		Angle			
2	1	95.012			
3	2	88.586			
4	3	46.597			
5	4	92.684	Number of Flocks	24	
6	5	42.285	Percentage	35.82	
7	6	105.111			
8	7	108.483			
9	8	85.39			
10	9	75.921			
11	10	63.733			
12	11	108.926			
13	12	121.195			
14	13	70.258			
15	14	136.102			
16	15	110.346			
17	16	42.103			
18	17	140.105			
19	18	95.695			
20	19	85.168			
21	20	110.566			
22	21	129.051			

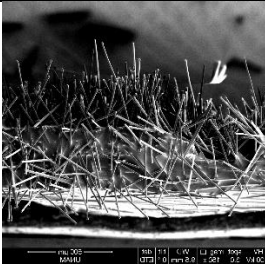
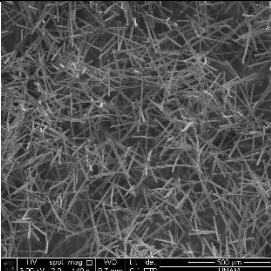
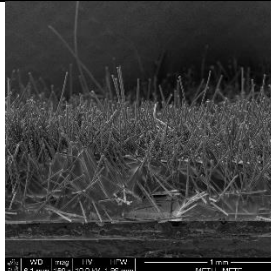
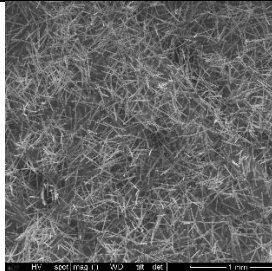
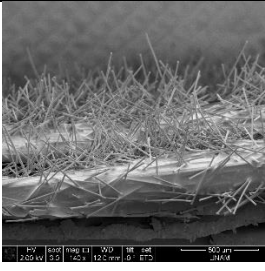
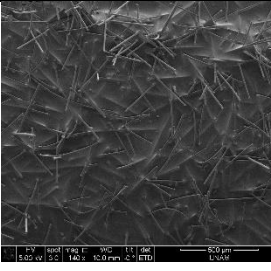
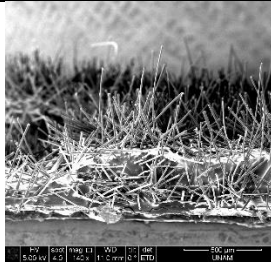
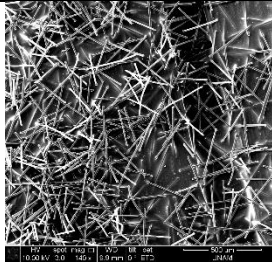
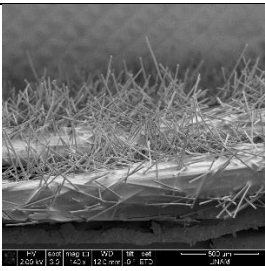
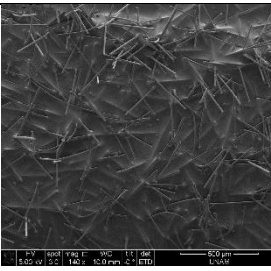
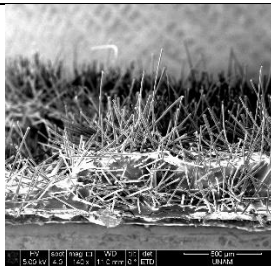
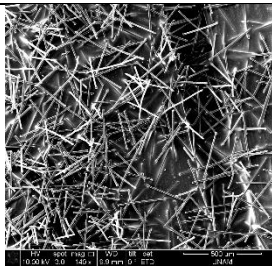
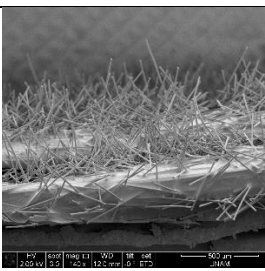
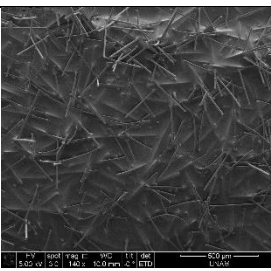
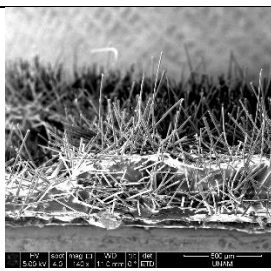
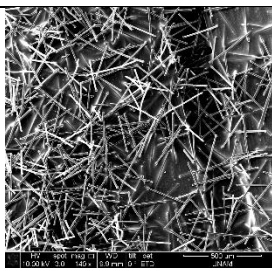
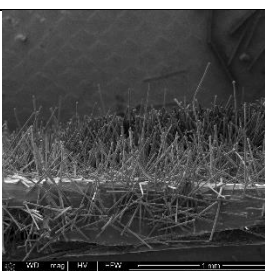
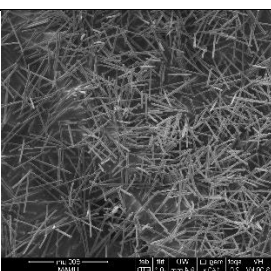
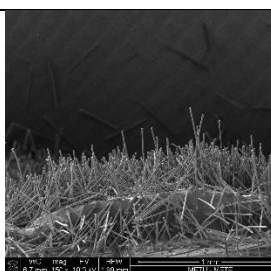
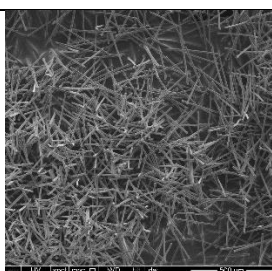
Figure 50 Vertical alignment calculation table.

The placement parameters (Density and VA) of 0.9 dtex 0.4mm flocks on the prepreg are given in the Table 6 and SEM images are given in Figure 52.

Table 6 Vertical alignment and density value of flocks

Sample No	Y	X	Voltage	Density (flocks/m)	VA (% population)
1	195	105	65	93	62.69
2	195	105	80	216	44.78
3	195	75	65	74	26.32
4	195	90	65	155	38.24
5	195	120	65	216	59.00
6	195	135	65	328	35.82
7	180	105	65	87	43.59
8	165	105	65	193	36.00
9	150	105	65	87	43.59
10	135	105	65	193	36.00
11	120	105	65	96	54.35
12	90	90	65	357	53.73
13	75	75	65	361	37.31
14	60	60	65	457	50.75
15	45	45	65	291	22.39



Side View of 5	Top View of 5	Side View of 6	Top View of 6
			
Side View of 7	Top View of 7	Side View of 8	Top View of 8
			
Side View of 9	Top View of 9	Side View of 10	Top View of 10
			
Side View of 11	Top View of 11	Side View of 12	Top View of 12
			
Side View of 13	Top View of 13	Side View of 14	Top View of 14
			

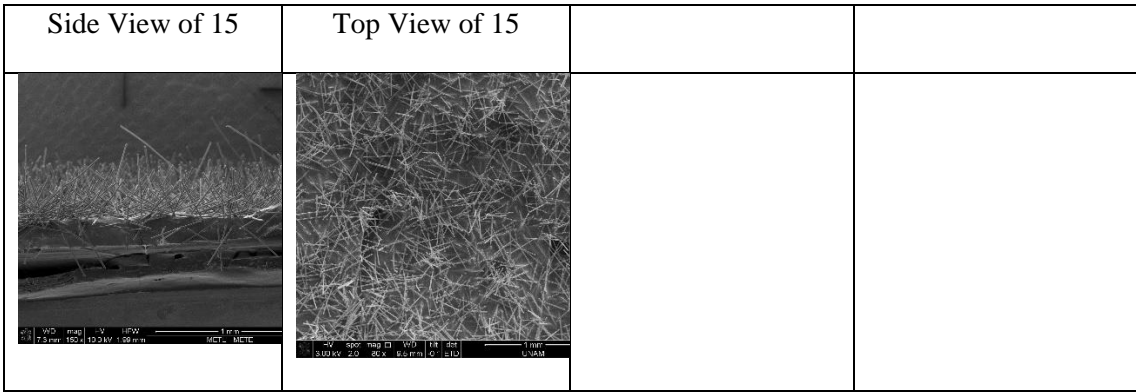


Figure 51 SEM images of flocked surface.

APPENDIX 3– Presentations from Thesis

M.Utku Yıldırım, Erhan Bat and Bora Maviş " Electrostatic Flocking of Small Sized Flocks " International Metallurgy and Materials Congress (IMMC'2021), 10-12 June 2021, Turkey. Poster Presentation.



Electrostatic Flocking of Small-Sized Flocks



Elektrostatik Floklama ile Küçük Boylu Flokların Floklanması

M.Utku Yıldırım¹, Erhan Bat², Bora Maviş^{1*}

¹Department of Mechanical Engineering, Hacettepe University, ANKARA

² Department of Chemical Engineering, Middle East Technical University, ANKARA

*Corresponding author, e-mail address: boramavis@gmail.com

ABSTRACT

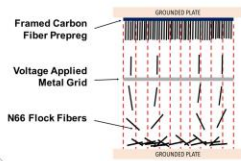
The electrostatic flocking, which is widely used in textile industry, has recently been used in advanced applications. This study is performed to investigate the experimental setup and process parameters required to position the short flocks perpendicular to the carbon fiber prepregs. The conductivity of the epoxy is much lower than the water-based adhesives used in the textile industry. Low conductivity requires the parameters to be more precisely adjusted for the vertical positioning of the flocks. In order to increase the vertical alignment of shorter flocks and control their surface density, applied voltage, application time and distances of the flock reservoir and the target to a grid placed in between them were varied.

INTRODUCTION

Electrostatic flocking has been shown to be a promising technique in advanced applications like interfacial toughening of layered composites. Although shorter flocks were more effective in increasing interfacial toughness, in these focused studies, the shortest flocks used have not been less than 1.3 and 0.6 mm for N66 and polyester flocks, respectively [1]. Moreover, the effect of areal density of the flocks on mechanical properties have not been studied in depth. In contrary to the generally sought high values for densities in commodity item coatings, a well-controlled areal density of flocks in these high and applications can be critical. For testing these hypotheses, the knowledge of electrostatic flocking of flocks with small feature sizes is essential. Previous studies show that positioning short flocks vertically is more difficult than taller [2]. Also, there is new studies on flow control of microfiber(0.54-2.53mm) flow control on the epoxy adhesive [3]. Here, we focus on the effect of experimental parameters that can possibly affect the density and vertical alignment of shorter flocks(0.4mm) on epoxy resin-carbon fiber prepregs.

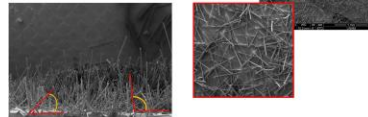
EXPERIMENTAL SETUP

- Carbon fiber prepreg is grounded with metal frame. In this way it is aim to discharge flocks on the surface.
- Framed prepreg located top and 0.4 mm N66 flocks are placed on the bottom grounded plate. Grid and prepreg location adjusted with brackets.
- Voltage is applied to the grid to place the flocks on the prepreg, and the flocks move along the electric field from the bottom plate to the prepreg.



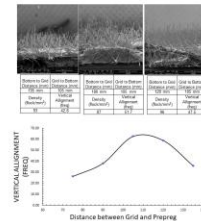
MEASUREMENT OF DENSITY AND FLOCK ANGLES

- The top view image was taken to measure the density. Flocks are counted within 1mm² of prepreg surface.
- The front view image was taken to measure angle of each flock and than frequency of angle between 75-90 degrees are calculated.



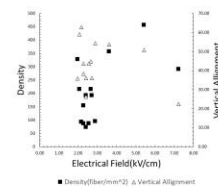
EFFECT OF DISTANCE BETWEEN GRID AND TOP PLATE

- 65 kV applied to the grid in all modifications while keeping the distance between the bottom and the grid constant.
- As distance increases electrical field decreases. So it is shown form graph, there is an optimal electrical field to get optimal vertical alignment on the surface.



EFFECT OF ELECTRICAL FIELD ON SURFACE DENSITY AND VERTICAL ALIGNMENT

- Flocks can be placed more vertically at different application distances in the same electric field.
- As electrical field increases surface density increases.



CONCLUSION & PERSPECTIVE

- As seen in previous studies, when the electrical force on the flocks is too high, the flocks stick to the surface in a slanted or oblique before they can be aligned vertically.
- Since the flocks come to the surface very quickly when the electric field is above a certain level, new flocks will meet with a charged surface and their vertical alignment will be disrupted before the flocks attached to the surface are discharged.

- The flocks coming from the back of the flocks that cannot be discharged may not be able to stick to the surface and after a certain fiber density, more flocks cannot stick to the surface.
- Grid to bottom distance and electrical field must be adjust together to allow time for the flocks to align vertical.

ACKNOWLEDGMENT

The authors acknowledge use of the services and facilities of UNAM-National Nanotechnology Research Center at Bilkent University and the financial support from TUBITAK (Project No: 214M110) and Hacettepe University (Project No: FYL-2020-18719).

REFERENCES

- [1] Kim, Y.K. and A. Lewis, Journal of Advanced Materials -Covina, 2017
- [2] Yu, Z., S. Wei, and J. Guo, Journal of Materials Science: Materials in Electronics
- [3] Hasegawa, M. and H. Sakaue, Sensors and Actuators A: Physical, 2020. 312: p. 112125.